UNIVERSITÀ DEGLI STUDI DI PADOVA

Corso di Laurea Magistrale in Bioingegneria

Dipartimento di Ingegneria dell'Informazione

Coupling of polymeric brushes functionalized with RGD peptide on PCL surfaces to increase cell adhesion

Relatore: Prof. Monica Dettin
(Dipartimento di Ingegneria Industriale)
Correlatori: Prof. Lorenzo Moroni,
Dr. Matt Baker, Khadija Mulder
(Maastricht University)

Laureanda: Sara Dallan
matricola 1129854

Anno Accademico 2017-2018

Sommario

L'osteoartrite è una malattia degenerativa della cartilagine articolare, la quale ha una limitata capacità intrinseca di auto-rigenerazione, portando alla formazione di difetti che possono intaccare sia la cartilagine che l'osso sottostante. Per creare un costrutto capace di sostituire e rigenerare questo particolare tessuto, un polimero biodegradabile funzionalizzato attraverso spazzole polimeriche può rappresentare un sostituto al danno della cartilagine. Per iniziare, lo scopo di questo lavoro è lo studio della funzionalizzazione di una superficie di polimero biodegradabile con un peptide bioattivo attraverso spazzole polimeriche. Perciò sono stati preparati film di policaprolattone (PCL) usando una pressa a riscaldamento. Le spazzole di poli(N-isopropilacrilammide) (PNIPAM), sintetizzate attraverso la tecnica di polimerizzazione RAFT (Reversible Addition-Fragmentation Transfer), sono state introdotte nella superificie attraverso il metodo di "grafting-to", sfruttando la presenza della maleimide nella superficie di PCL. Presenza confermata utilizzando la fluorescenza di BSA-FITC. L'introduzione delle spazzole di PNIPAM è stata confermata dall'analisi FT-IR, con un segnale crescente per le maggiori percentuali di maleimide. Le spazzole di PNIPAM contengono un gruppo finale aldeidico, utilizzato per l'introduzione del peptide RGD, attraverso la reazione con il gruppo amminoossilico del peptide. Inoltre, l'introduzione delle spazzole polimeriche e del peptide è stata ripetuta in presenza di un catalizzatore. Infine, le cellule di osteosarcoma MG 63 sono state seminate su film funzionalizzati, per testare l'influenza di ogni componente: maleimide, spazzole di PNIPAM and peptide RGD. I risultati della semina cellulare, ottenuti con la colorazione DAPI e falloidina 488, mostrano che la presenza del peptide RGD aumenta l'adesione cellulare nelle superfici funzionalizzate dopo 3 giorni, con un maggior numero di cellule all'aumentare della percentuale di maleimide. Il solo PCL presenta un andamento quasi costante nel numero di cellule durante l'esperimento, manifestando il bisogno di una funzionalizzazione superficiale per migliorare le caratteristiche del materiale per questa applicazione.

Abstract

Osteoarthritis is a complex disease referring to the degeneration of articular cartilage, which has poor intrinsic capacity of self-regeneration, leading to creation of defects, which can affect both cartilage and underlying bone. In order to find a way to create a construct able to replace and regenerate this particular tissue, a functionalized biodegradable polymer via polymer brushes can represent a design for cartilage loss. To begin with this idea, the aim of this work is the study of the functionalization of a biodegradable polymer surface with bioactive peptide via polymer brushes. Therefore, films of polycaprolactone (PCL) were prepared using hot press. Poly-(N-isopropylacrylamide) (PNIPAM) brushes, synthetized via reversible addition-fragmentation chain transfer (RAFT) polymerization, were introduced on the surface via "grafting-to" technique, exploiting the presence of maleimide on PCL surface. This was confirmed using BSA-FITC staining. FT-IR analysis show the successful introduction of PNIPAM brushes, with increasing signal for higher percentages of maleimide. The PNIPAM brushes contained an aldehyde end-group, employed for the introduction of the RGD peptide, which was synthetized containing an amino-oxy group: the coupling between the brushes and the peptide occurs through an aldehyde - amino-oxy reaction. Furthermore, the introduction of brushes and peptide was repeated in presence of a catalyst. Lastly, functionalized films were seeded with MG 63 osteosarcoma cells, to test the influence of each component: maleimide, PNIPAM brushes and RGD peptide. The results on the seeded samples from DAPI and phalloidin 488 staining showed that the presence of RGD peptide increases cell adhesion on surfaces with functionalized PNIPAM brushes on day 3, with higher number of cells as the percentage of maleimide increases, while the presence of only PNIPAM brushes does not increase the cell number on the samples. PCL itself presents almost a constant number of cells after the modifications of the surface, revealing the requirement of a functionalization of the surface to improve the features of the material for this application.

Contents

Chapter 1

Introduction

1.1 Osteoarthritis

Degeneration of mature articular cartilage is the major cause of disability and it can be caused by a trauma or during the course of joints disorders such as osteoarthritis (OA) [1, 2]. Osteoarthritis is the main form of arthritis [3] and it is a complex disease that affects millions of people worldwide [4]. The incidence of this disease is increasing with increased life expectancy and rising levels of obesity [5]. OA is predicted to become the fourth cause of disability worldwide by 2020 [6]. Severe joint pain and loss of function characterized the osteoarthritis, resulting in difficulties in daily activities and affecting the quality of life [7]. The sites that are most affected by OA are knee, hip and hand [5]. Furthermore, osteoarthritis is associated with a considerable socioeconomic cost, relating to not only medical cost but also cost of work absence and early retirement [4, 6].

During the course of the osteoarthritis, the components of the articular cartilage show morphological, structural, biochemical and biomechanical changes, which imply the degeneration and loss of the cartilage tissue [8]. A comparison between healthy and OA tissue is represented in Figure 1.1, showing the cartilage of the knee as an example. The healing of damaged articular cartilage is complicated, due to its poor intrinsic capacity of repair and self-regenerate. Articular cartilage is an avascular tissue and it does not response to an injury following the usual cascade of events of inflammatory reaction, common to other tissues. There is no cure for the osteoarthritis. Conventional osteoarthritis treatments aim at pain and weight management and improving the function, with surgical procedures for end-stage disease.

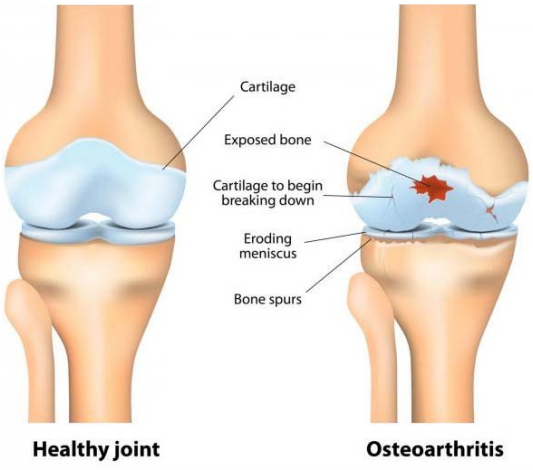

Figure 1.1: Healthy and OA knee joint [9]

Moreover, the surgical intervention induces a fibrous repair tissue, which is a different tissue than the healthy articular cartilage [7]. For this reason, strategies involving tissue engineering are developing in order to promote cartilage tissue regeneration [2]. The challenge within this tissue is the repair of the osteochondral interface, developing a structure able to regenerate the cartilage and to integrate with the underlying bone [3].

In order to understand how osteoarthritis phenomena acts on the cartilage tissue and the underlying bone, and how to develop a structure able to regenerate the interface between these two tissues, it is important to know the composition, the structure and the function of the tissues under discussion.

1.2 Bone tissue

Bones are vascularized and innervated organs, consisting of bone tissue, bone marrow and a surrounding connective tissue. The principal functions of the bone tissue include support of softer tissues, such as muscles, allowing the movement, protection of internal organs, production of blood cells and storage of minerals, in particular calcium and phosphorous [10].

Bones can be classified, according to their shape, into long bones, short bones and flat bones. In particular, the long bones are employed to describe the macroscopic structure of the bone [11]. An adult long bone consist of a diaphysis, the central part of the bone, and two epiphysis, localized at the ends of the bone. The structure of the bone differs in the two compartments just described, as shown in Figure 1.2: the diaphysis is composed mainly

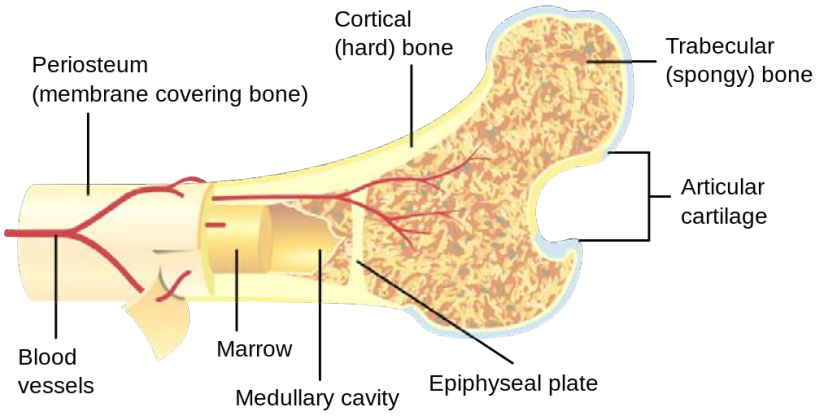

Figure 1.2: Cortical and trabecular bone [12]

of cortical bone, which represents the external part of the bone, while the inner part of the diaphysis and the epiphysis consist mostly of cancellous or trabecular bone [13]. On the joint surfaces, at the end of epiphysis, a thin layer of articular cartilage covers the subchondral bone. Cortical bone is a dense and highly mineralized bone tissue that constitutes 80% of the mass of the bone tissue in the body and it is largely responsible of mechanical and structural properties of the bone [10]. The remaining 20% of the bone mass is represented by trabecular bone, a porous structure composed by a lattice of plates and rods known as trabecula [11]. In the bone marrow channel, the inner central part of the bone, the space between the trabecula becomes wider and filled with bone marrow [10].

Bone is a mineralized connective tissue, composed of mineral, organic matrix, cells and water [14]. The mineral content consist mostly of hydroxyapatite $Ca_{10}(PO_4)_6OH_2$ [11]. Type I collagen is the major component of the organic matrix, containing also non-collagenous proteins, such as osteocalcin, osteopontin, osteonectin and bone sialoprotein [15]. The cells involved in the formation, modelling and remodelling of the bone are osteoblasts, osteoclasts, and osteocytes. The precursor of these cells is constituted by mesenchymal stromal cells (hMSCs), which represent a small fraction within the bone marrow. Osteoblast are responsible of bone synthesis and deposition, while osteoclasts are responsible of bone resorption. These opposite activities of osteoblasts and osteoclasts are regulated by hormones, based on the calcium request from the body. In addition, the interactions of the process between osteoblasts and osteoclasts are controlled by the third type of cells, the osteocytes. These cells are actively involved in maintaining the bone matrix, but they are also mechanotransductors, allowing the transmis-

sion of signals via mechanical, electrical and chemical mechanisms [13].

The structure and the composition of bone tissue differs significantly from the cartilage tissue, described in the following section.

1.3 Articular cartilage

Hyaline cartilage, or articular cartilage, is a highly specialized connective tissue that cover the gliding surfaces of diarthroidal joints [16]. It is a low friction tissue, with a high capacity to bear and distribute loads and it permits the movement of articulating bones [17]. Hyaline cartilage has unique mechanical behaviour, but it has limited capacity for healing and repair. Articular cartilage lacks of blood vessels, nerves and lymphatics and, once damaged, it cannot have the usual inflammatory response experienced by other vascularized and innervated tissues [18]. Hyaline cartilage is made of a dense extracellular matrix (ECM) with sparse population of highly specialized cells, the chondrocytes. The ECM is composed primarily of water, collagen and proteoglycans, with smaller amount of noncollagenous proteins and glycoproteins. Water is the main fluid component of the articular cartilage and it represents 80% of its wet weight. Since the cartilage tissue has no vascularity, the presence of water allows the transport and the distribution of nutrients to chondrocytes. In addition, water provides lubrication of the tissue. Collagen is the most abundant macromolecule and forms 10-20% of the wet weight of the articular cartilage. Collagen II represents the predominant type of collagen within the ECM. Collagen creates a network with a well-defined ultrastructure, in which the orientation of the fibers changes with the depth of the articular cartilage. It provides tensile and shear stiffness and strength of cartilage tissue [16, 19]. Proteoglycans represent the second-largest group of macromolecules in the ECM, up to 10-15% of the wet weight of the cartilaginous tissue. Proteoglycans are embedded within the collagen network, creating a fiber-reinforced material. They provide a compressive strength to the articular cartilage. Chondrocytes derive from mesenchymal stem cells, they are only 1-5% of the volume and they are sparsely distributed within the ECM. They are responsible of the synthesis of the components of the extracellular matrix and they regulate the maintenance and the metabolism of the matrix [20]. All these components vary with the depth of articular cartilage. The tissue can be divided in four different zones, showed in the Figure 1.3: the superficial zone, the middle zone, the deep zone and the calcified zone. The superficial or tangential zone is the thinnest layer, that is characterized by densely packed collagen fibers that are oriented parallel to the articular surface. This zone has a low concentra-

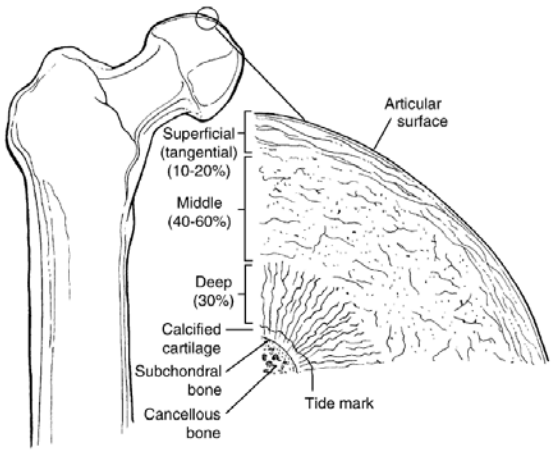

Figure 1.3: Articular cartilage layers

tion of proteoglycans and a low permeability. The chondrocytes are present in relatively high number, they have flattened ellipsoid shape and they are oriented along the collagen fibers. This layer has the highest water content. The integrity of this layer is important for the protection and maintenance of the deeper layers. The arrangement of the collagen fibers provides the greatest tensile and shear strength. Changes in the structure of this zone alters the mechanical properties of the cartilage and contribute to the development of osteoarthritis [20] . The middle or transitional zone represent an anatomic and functional bridge between the superficial and the deeper zones. This layer is characterized by higher concentration of proteoglycans and a lower concentration of chondrocytes, which have a more spherical shape. In this region, the collagen fibers have an arcade-like structure interspersed with randomly oriented fibers. This zone represent the first line against the compressive forces. The following layer is the last region of purely hyaline tissue before reaching the bone and it provides the greatest resistance to compressive force [16]. In the deep zone, the collagen fibers are oriented perpendicular to the articular surface and anchored to the underlying subchondral bone. This region is characterized by the highest proteoglycans content and the lowest water content and cell density. Chondrocytes are slightly elongated and oriented in the direction of the collagen fibers. The border between the deep zone and the calcified zone is called “tidemark”. The calcified zone contains a poor concentration of chondrocytes, embedded in a calcified matrix. The cells are hypertrophic and synthetize type X collagen, which provides structural integrity and a shock absorber along with the

subchondral bone [20]. This layer of mineralized cartilage matrix represents the osteochondral interface, which links the articular cartilage tissue to the underlying subchondral bone [3]. In fact, this represents an anchorage point for the cartilage tissue. The characteristics of the components of articular cartilage makes it a fluid-saturated, fiber-reinforced, porous and permeable composite material [17]. Besides the complex structure, the articular cartilage lacks the intrinsic ability to regenerate, as it is an avascular tissue. For this reason, cartilage is not able to self-repair after a traumatic injury or to contain the process of osteoarthritis and consequently to obtain the restoration of its structure and function [20].

The defects in the articular cartilage are classified based on their depth and they can be divided in chondral or osteochondral. The first type of defect refers to a lesion of the articular cartilage alone, whereas the second one represents an injury of the articular cartilage together with the subchondral bone [19]. The difference between the articular cartilage defects is shown in Figure 1.4, where chondral defects are represented by the partial-thickness and full-thickness cartilage defects, whereas the bone-cartilage defect represents the osteochondral defects.

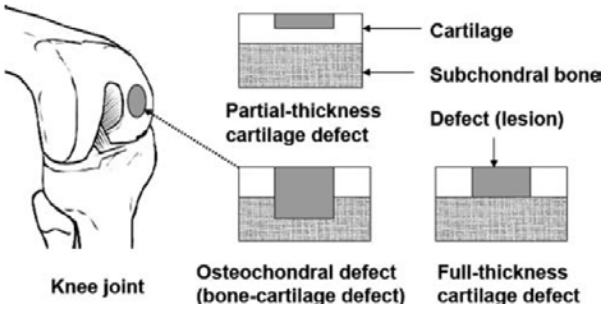

Figure 1.4: Chondral and osteochondral defects of articular cartilage [21]

Besides the treatments for relieving the pain, there are also surgical interventions including subchondral stimulation, mosaicplasty and periosteal grafts [3]. However, all these strategies give suboptimal results. An alternative approach, which is developing in the last years, is given by tissue engineering.

1.4 Tissue Engineering

The term "Tissue Engineering", as recognized today, was introduced at a bioengineering panel meeting of the National Science Foundation in 1987. This led to the first meeting focused on the subject of tissue engineering

the following year [22]. Tissue Engineering is an interdisciplinary field that applies the principles and innovations of engineering and life science to the development of biological substitutes in order to restore, maintain or improve an organ or a tissue function [23]. The loss of part of an organ or a tissue, compromised or removed because of accidents, tumor or trauma, is one of the most frequent, devastating and costly problems in human health care and the ultimate goal of the surgery is the repair of the damaged tissue or organ. The most commonly used methods are tissue grafting and organ transplantation or synthetic material replacement [24]. The limitations of the first method include the cost of the transplantation, the donor shortage and the possible long-term problems after the transplantation. The second one gives poorly integration with the host tissue and failure over the time [25]. The goal of the field of tissue engineering is to overcome the limitations of these conventional treatments for damaged tissue or organ, producing substitutes that can grow with the patient, without needing a second surgery or supplementary therapies and in the end, making this solution a cost-effective treatment in the long term [26]. The key components of tissue engineering, that promote the achievement of the goals of this new field, are scaffolds, cells and bioactive molecules. These elements can be combined in a suitable biological environment to produce engineered tissue in vitro or used as a strategy of tissue regeneration in vivo [21]. The combination of these elements is generally referred to as tissue engineering triad (Figure 1.5).

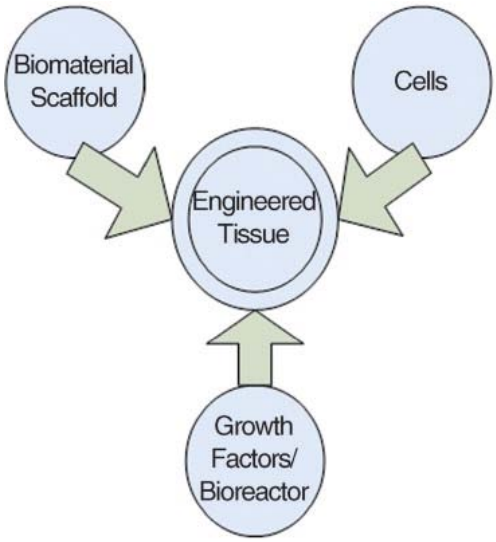

Figure 1.5: Tissue engineering triad [27]

1.4.1 Scaffolds in Tissue Engineering

In general, tissue engineering involves the development of a three-dimensional scaffold that provide the environment to support and guide the growth and the proliferation of cells, promoting the formation of new tissue [28]. It is possible to create a new tissue, using this approach, with which the body can interact and carry out all the expected biological activities. In this way, the created scaffold will have tailored and biomimetic properties [29]. The successful tissue engineered scaffold has to satisfy many requirements:

- its structure has to be three-dimensional, with sufficient porosity and adequate pores shape and size to promote tissue integration and vascularization,
- it has to be made of material that is biocompatible, with controlled biodegradability and that function without interrupting other physiological activities,
- it should have appropriate surface chemistry in order to promote cells adhesion, differentiation and proliferation,
- it needs to have the adequate mechanical properties that match the properties needed by the tissue in the site of implantation,
- it must not promote adverse response and
- it has to be easy to fabricate in a variety of configurations [23, 26].

Furthermore, the rate of degradation of the scaffold has to be close to the regeneration rate of the desired natural tissue [29].These aforementioned characteristics refer to the architecture and the material of the tissue-engineered scaffold. In addition to these components, cells able to differentiate in the specific cell phenotype and bioactive substance giving the stimulus for the differentiation are required for the success of the tissue engineering [30]. Ideally, a scaffold should be able to mimic the structure, the composition and the biological function of the natural extracellular matrix and its mechanical support so as regulate the cellular activities [31].

The materials used for the fabrication of the scaffold should be biocompatible, biodegradable and bioresorbable. In addition, degradation products should be removed from the body via metabolic pathway, without adverse response and an adequate rate. The most used materials in tissue engineering are:

- naturally derived materials, such as collagen
- acellular tissue matrices
- synthetic polymers
- ceramics

The advantages of natural materials are their biological recognition, the sharing of mechanical, chemical and physical properties of the replacing tissue, but the high cost of these materials is a limiting factor for their use. As for the synthetic materials, they can be reproduced on large scale, they are cost efficient and it is possible to tailor the mechanical and physical properties to the application, but they usually lack of recognition sites to communicate with the cells [32]. The most commonly used synthetic materials are biodegradable polymers, in particular

- polyglicolic acid (PGA)
- polylactic acid (PLA)

  and their copolymers (PLGA)
- polycaprolactone (PCL) [33]

1.5 Biodegradable polymers

The definition of a biomaterial includes any natural or synthetic materials that can be engineered in order to interact with biological systems without causing any adverse reactions. Within the group of the biomaterials used in medical applications, polymers have a great importance. A particular subgroup of these biomaterials are the biodegradable polymers. They gain interest because these polymers can be broken down and excreted or resorbed without the needing of a second surgery to remove them [34]. In the recent years, many polymeric biomaterials with different properties has been investigated and developed for tissue engineering applications. Many of these biomaterials show desired biodegradation properties and good mechanical properties. One challenging regarding polymeric materials in medical applications is that they lack of interactive properties with the cells [35]. This limitation can be solved with the application of a surface modification technique on these biomaterials. In this way, it is possible to improve cells interactions with the substrate, maintaining the other characteristics of the biomaterials [36]. Many of these techniques are focused on the immobilization of biomolecules onto the surface of the scaffold [31].

1.5.1 Polycaprolactone

Polycaprolactone (PCL) is an aliphatic biodegradable polyester of liner formula $(C_6H_{10}O_2)_n$ with a semicrystalline structure. It is biocompatible, bioresorbable and characterized by a melting temperature T_m of ca 60°C and a glass transition temperature T_g of ca -60°C. PCL is a FDA-approved biomaterial, it has good mechanical properties and it has exceptional ability to form blends. Furthermore, PCL degrades at slower rate than the other polymers (2-3 years). PCL is one of the early polyester synthetized by the Carothers group in the 1930s. In the 1970s-1980s PCL and its copolymer were extensively used, in particular in the field of drug delivery. Due to its slow degradation rate, it was replaced in the following years by other resorbable polymer, more suitable for a few months' applications. Thanks to the development of the field of the tissue engineering, in the last years PCL regain importance, being extensively investigated as a scaffold material [37, 38]. However, beyond its slow degradation rate, its biocompatibility, the easily fabrication and the appropriate mechanical properties, the major drawback of the PCL is its hydrophobic nature and consequently, the absence of biologic recognition sites. Several surface modification techniques have been investigated in order to overcome these limitations and improve the cell adhesion and proliferation and the biocompatibility of this polymer [36].

1.6 Functionalization of surfaces

Biomaterials show appropriate bulk properties for their end use in biomedical applications, but sites of interactions with the biological environment are not always present on the surface of the biomaterial. This is a limitation, because communications between a biomaterial and its surrounding occur through the interfaces. Several surface modification techniques have been developed in order to design a material that can have specific, desirable and biological interactions with the surroundings. In the last 50 years, there was a dramatic progress in the ability to understand and to characterize these interactions, but also to comprehend molecular mechanisms and signalling between cells and their environment. Consequently, knowledge of material surface science, and cell and molecular biology are needed to arrange and control the interactions at the interfaces of a successful biomaterial [39].

Chemical and physical surface modifications approaches for the functionalization of the interface have recently gain importance as promising methods to tailor chemical, physical and biological properties of the sub-

strates in order to increase the adhesion, proliferation and differentiation of the cells [40]. The methods of surface modification allow the introduction of specific functional groups, which can be used to tether a bioactive compound to a substrate via a spacer molecule. Functional groups commonly used in bioconjugation are thiols, aldehydes, carboxylic acids, hydroxyls and primary amines. In Figure 1.6 it is shown the procedure of functionalization with a polymeric substrate.

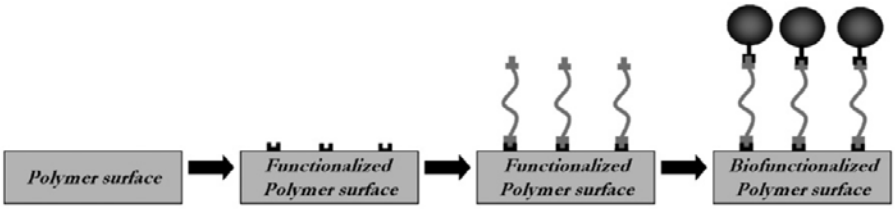

Figure 1.6: Concept of biological surface modification [41]

In this functionalization strategy, the spacer molecule can be given by a tethered polymeric species that can be assembled, grown or grafted onto the substrate via covalent or physical interactions. These assemblies are called polymer brushes and they can be applied to both metallic and polymer substrates [40]. These layers consisting of polymer brushes can also be used to modulate the properties of the surface without affecting the bulk properties of the material [42].

1.6.1 Polymer brushes

Polymer brushes is the term used for polymer chain end-grafted to a supporting surface [43]. The presence on a surface of this thin polymer layer can affect its properties such as wettability, adhesion, lubrication, friction and biocompatibility [42]. The advantages of polymer brushes, compared to other surface modification methods, are their mechanical and chemical robustness [44], and the possibility to control various important architectural features: the length of the polymer chain, the grafting density, the thickness of the polymer coating and the chemistry of the brushes [45]. In addition, the flexibility to introduce different functional groups [44].

The covalent grafting of polymer brushes to the surface can be accomplish by two different approaches, named “grafting-to” and “grafting-from” techniques. “Grafting-to” method involves a chemical reaction between preformed, end-functionalized polymers and substrate, where complementary functional groups are located, resulting in tethered polymer brushes [46].

The addition of polymer brushes with this approach is experimentally simple and it is possible to characterize accurately the preformed polymer via chemical and physical methods [42], but it has some limitations. It is difficult to produce a thick layer of polymer and to achieve high grafting density [44]. The latter limitation is due to the steric hindrance, caused by the previously attached polymers, which block the remaining binding sites present on the surface [47]. "Grafting-from" technique involves the formation of the polymer chain via polymerization from initiators [48], usually covalently bonded to the surface. This approach, which initiate the growth of the chain directly on the surface, allows obtaining higher grafting density. The complications of this method can be the efficiency of the initiator, its presence on the surface [43].

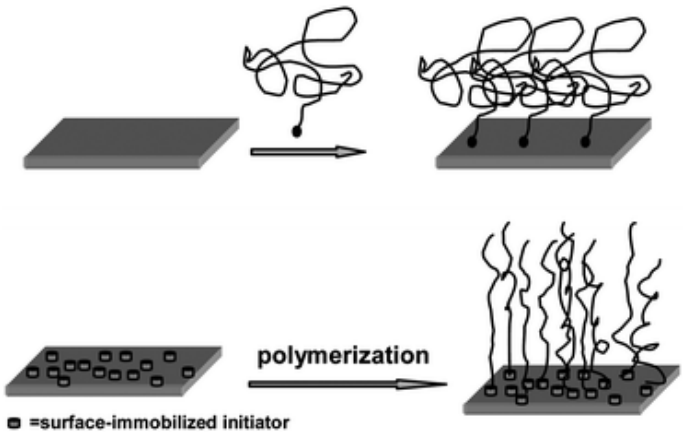

Figure 1.7: Representation of "grafting to" and "grafting from" methods [49]

The introduction of polymer brushes as surface coating method has recently gain attention in the fields of stem cell biology, tissue engineering and regenerative medicine. This is due not only to the easy fabrication process and the compatibility with different materials, but also to the simplicity of coupling bioactive molecules to polymer brushes [48]. In this way, the presence of bioactive materials can influence cell adhesion, formation, proliferation and differentiation.

1.6.2 Bioactive peptides

The cell adhesion on a surface is mediated by the interactions between the receptors on the cell membrane and their ligands, such as peptides, proteins, saccharides and other biologically active substances [50]. At the beginning, the functionalization of surfaces were done using cell adhesive proteins, but

the use of proteins has some disadvantages. First, the proteins have to be isolated from other organisms and purified. They may cause undesirable immune response and increase the risks of infections. In addition, the proteins can undergo to proteolytic degradation and they have to be continuously refreshed, and this would be impossible for long-term applications. Most of these limitations can be overcome by using a smaller sequence of a peptide, containing the cell recognition motif of the protein. The advantages of the peptides are the higher stability towards sterilization conditions, heat treatments and pH variation, easy characterization and cost effectiveness. In addition, the smaller size of the peptides allows packing them with higher density, compensating the possibly lower cell adhesion activity [51].

Bioactive peptides are sequences of amino acids that mimic the functions of biological molecules. In particular, of the molecules present in the extracellular matrix (ECM) [47]. In general, a peptide that contains the cell-binding domain of an ECM protein is immobilized on the surface; the receptors found in the cell membrane recognize its ligand and bind to it. In this way, the ligand-receptor interactions promote the cell adhesion on the surface [50].

The most employed adhesion peptide is the sequence of RGD, derived from the cell-binding domain of the fibronectin, an ECM protein.

1.6.2.1 RGD sequence

The RGD sequence (R: arginine, G: glycine, D: aspartic acid) was identified in 1984 by Pierschbacher and Ruoslahti as a cell-binding region in fibronectin [52]. Fibronectin is a protein of the extracellular matrix that promotes cell attachment and spreading. The recognition of the RGD domain in the fibronectin is the major mechanism for the adhesion of anchorage-dependent cells [50]. Since the discovery of the RGD motif, various materials have been functionalized using this sequence, for medical studies and applications. The presence of the RGD peptide not only stimulates cell adhesion, but it has also the ability to address certain cell lines and to increase specific cell responses. Besides RGD sequence, other cell adhesion motifs have been identified, found on ECM proteins, soluble proteins and natural or synthetic peptides and they can be used in combination with RGD peptide or independently [51].

1.7 Aim of the thesis

The aim of this thesis is the functionalization of polymer surfaces with a bioactive peptide, through the specific coupling with polymer brushes. The

material used for making the surfaces is a biodegradable polymer, polycaprolactone and the choice of this polymer is given by the intended applications for the particular construct, which are the reparation and regeneration of the articular cartilage tissue. The addition of the polymer brushes gives the possibility to modify the surface of the material. In the bioactive peptide, containing the RGD sequence, is present a particular functional group, used for the specific coupling with the polymer brushes.

First, 2D surface of polycaprolactone (PCL) are made; then, polymer brushes are added to the surface, using a specific coupling between the polymer brushes and a compound mixed with PCL, the maleimide. At the end, the polymer brushes, through an aminoxy-aldehyde reaction, are functionalized with a peptide of sequence GRGDSP. After the preparation and the functionalization of the PCL surface, the influence of all the components on the adhesion and proliferation of cells is studied. For this purpose, various samples are seeded with MG63 osteosarcoma cells for different time points. The prepared surfaces are characterized using FTIR, GPC and contact angle. The cell studies are performed using fluorescent dyes and analysing microscopy images.

The GRGDSP peptide was prepared in the laboratory of chemical bioengineering at University of Padova, while the preparation of the material, functionalization and cell work were performed in the laboratories of MERLN Institute, Maastricht University.

Chapter 2

Materials and Methods

2.1 Materials

2.1.1 Materials and reagents

Materials and reagents provided by Sigma-Aldrich (Steinheim, Germany):

- 1,4-dioxane
- 1,6- hexanediamine
- 2-propanol
- BSA-FITC
- DAPI
- Diethyl ether
- DMF
- DMSO
- Ethylenediamine
- *m*-phenylenediamine
- Ninhydrin
- PBS
- Polycaprolactone - average $M_n = 45,000$

- TEA
- Trypan Blue

Materials and reagents provided by Thermo-Fisher Scientific (Waltham, MA, USA):

- Alexa Fluor™ 488 Phalloidin
- EZ-Link™ Alkoxyamine-PEG4-Biotin
- Gibco™ Trypsin-EDTA (0.05%), Phenol red
- MEM α, GlutaMAX™ Supplement, no nucleosides
- Penicillin-Streptomycin

Materials and reagents provided by VWR International (Radnor, PA, USA):

- BSA
- Ethanol
- PFA
- Potassium phosphate dibasic
- TCEP
- Triton® X-100

Materials and reagents provided by TCI Chemicals (Tokyo, Japan):

- 4-Amino-3-hydrazino-5-mercapto-1,2,4-triazole (Purpald®)
- 4-Amyloxybenzaldehyde
- Carboxymethoxylamine Hemihydrochloride
- N-(2-Hydroxyethyl)maleimide

2.1.2 PNIPAM

Poly(N-isopropylacrylamide), abbreviated PNIPAM, is a thermoresponsive polymer, used as material for the polymer brushes. It was prepared in the laboratories of MERLN Institute, at Maastricht University, by my daily supervisor Khadija Mulder.

2.1.3 RGD peptide

The functionalization of the samples in this work is done using a bioactive peptide, containing the RGD sequence. The peptide was synthesized in the laboratory of chemical bioengineering of the department of Industrial Engineering (University of Padova). The sequence of the peptide is

Aoa7 GRGDSP

where

- Aoa = amino-oxy-acetic acid
- 7 = 7-aminoheptanoic acid
- G = glycine
- R = arginine
- D = aspartic acid
- S = serine
- P = proline

and its molecular weight is MW=784.8 Da. The chemical structure of the peptide is shown in the following Figure 2.1:

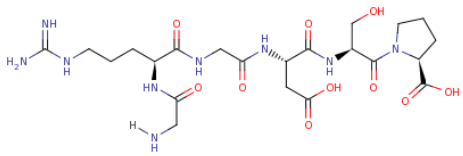

Figure 2.1: RGD peptide chemical structure [53]

2.1.4 MG 63 osteosarcoma cells

In this work, the samples are seeded with MG 63 osteosarcoma cells, provided by ATCC (American Type Culture Collection). These cells are highly proliferative and receptive for genetic manipulation; for their properties, MG 63 cells are widely used as in vitro models.

2.2 Methods

2.2.1 FT-IR

Fourier transform infrared spectroscopy is a technique used to obtain an absorption infrared spectrum of a compound. The functionality of this type of spectroscopy is based on the principle that almost all the molecules absorb infrared light. The spectrum derived from the measurement is characteristic of the sample and it represents the molecular "fingerprint" of the sample. Each substance has its own spectrum and two different molecular structure cannot share the same spectrum. FT-IR spectroscopy is used for identification, analysis of the structure of a variety of compounds, both organic and inorganic substances [54]. It is also useful for qualitative and quantitative analysis of a sample.

The instrumentation used in FT-IR spectroscopy is given by a spectrometer, whose basic components are:

- infrared source, which emits the radiation
- Michelson interferometer that modulates the infrared radiation
- detector, used to collect the IR beam that is passed through the sample
- computer that run the Fourier transform of the digitized signal.

The role of the Fourier transform is to convert the raw data in the final spectrum that is possible to analyse.

Figure 2.2 represents a scheme of the core of the spectrometer, the Michelson interferometer. The energy from an infrared source passes through

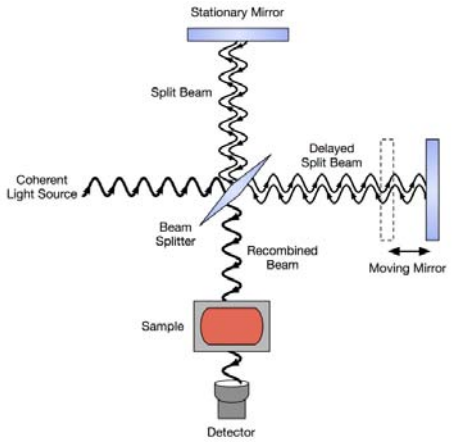

Figure 2.2: Michelson interferometer

a beam splitter, which divides the incoming radiation in two perpendicular beams. One beam is directed towards a fixed mirror, while the other beam goes to a moving mirror. The two beams recombine at the beam splitter, but the differences in the pathlength between the beams cause constructive and destructive interference. The combined beam is called interferogram. The infrared (IR) radiation, coming from the beam splitter, hit the samples and when it passes through it, some of the radiation is absorbed and some of it is transmitted, as it passes through the sample. The signal, which is collected by the detector of the FT-IR spectrometer, is the spectrum that results from the interaction between the IR radiation and the analysed spectrum [55].

The region of electromagnetic spectrum interested in the FT-IR analysis is the infrared region, in particular the vibrational portion of this region. In chemistry, it is preferred to express the radiation in this vibrational infrared region using the unit called wavenumber $\bar{\nu}$. The wavenumber can be easily calculate as the reciprocal of the wavelength and it is expressed in cm^{-1}. Using the wavenumber, the vibrational infrared spectrum extends from 4000 to 400 cm^{-1} . Almost any compound with covalent bonds absorbs electromagnetic radiation in the infrared region. The IR radiation produces different types of vibrations and rotations of the covalent bonds between two elements. The simplest types of vibrational motions that a molecule can experience are the stretching and the bending modes. The first one is the continuously changing of the interatomic distance along the axis of the bond between two atoms. The stretching mode can be symmetric or asymmetric. The second type of vibrational motion occurs when the angle between two bonds changes. There are various bending modes named wagging, twisting, scissoring and rocking [56].

2.2.2 GPC

Gel permeation chromatography is a technique that separates analytes based on their size. The mechanism of GPC involves the injection of dissolved molecules onto specialized columns, containing packed porous beads. GPC columns can contains pores of single size or of different sizes. The degree of access of the molecules to the pores determines the separation process. The smaller molecules can easily access the pores and they can spend more time in the column, whereas larger analytes are restricted in available pores or they are excluded from the pores, and they are eluted quickly. The samples leaves the column in the inverse order of molecular size, as shown in Figure 2.3; the largest molecule is the first to leave, followed by progressively smaller molecules.

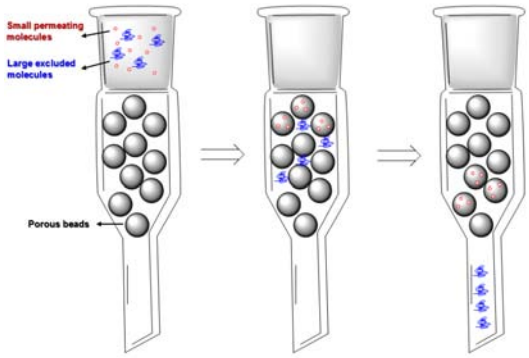

Figure 2.3: GPC mechanism [57]

In order to analyse the sample, this has to be prepared. The preparation of the sample consists in the dissolution of the sample in an appropriate solvent, filtration of the obtained solution and its injection onto a column. The material eluting from the column reaches the detectors of the GPC. The most widely used is the differential refractometer (RI detector) that measures the difference in refractive index between the solvent and the sample + solvent. It determines the amount of eluted material as a function of the retention time, converted to molecular weight using a calibration curve, generated using polymers of known molecular weight, which relates the retention time with the molecular weight of the polymer. In addition, the photodiode array (PDA) detector can be present, which can look at a range of wavelengths and it allows determining information about the chemical composition distribution.

GPC is a valuable tool used to determine the molecular weight of a sample as well as the distribution of the molecular weight. The analyzed samples of this technique are usually polymers, that are characterized by different molecular weight definitions. GPC can be used to determine the following molecular weight averages:

- Number average molecular weight M_n, that is the statistical average molecular weight of all the polymer chains

$$M_n = \frac{\sum N_i \cdot M_i}{\sum N_i}$$

- Weight average molecular weight M_W

$$M_W = \frac{\sum N_i \cdot M_i^2}{\sum N_i \cdot M_i}$$

- Size average molecular weight M_Z

$$M_Z = \frac{\sum N_i \cdot M_i^3}{\sum N_i \cdot M_i^2}$$

  where M_i is the molecular weight of a chain and N_i is the number of chain of that molecular weight

- Polydispersity index PDI, that represents the broadness of the molecular weight distribution. It is given by the following ratio:

$$PDI = \frac{M_W}{M_n}$$

At the end of the measurement performed by the GPC, the obtained output is a chromatograp, showed in Figure 2.4.

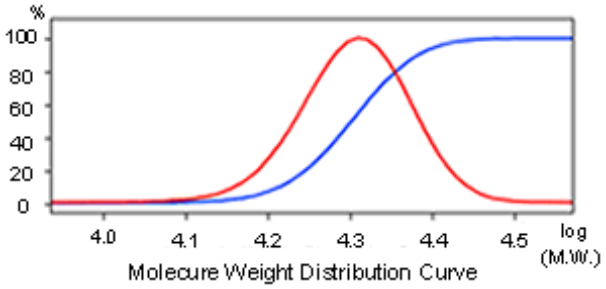

Figure 2.4: Example of molecular weight distribution

2.2.3 Contact angle

Contact angle is a useful and simple technique to analyse surface properties, in particular, it directly measures the wettability of a surface. The wettability is a useful parameter in the study of the interactions between the surface of the material and the biological environment. Contact angle methods are inexpensive and easy to perform. The measurement is performed using a still drop of liquid on a surface and detecting the angle θ_C formed between the surface of the drop and the surface of the material. When the surface is wettable, the liquid drop tends to extend itself on a flat surface, whereas the drop forms a round shape when the surface is not wettable. In practice, when

- $\theta_C = 0$, the surface is completely wettable
- $0 < \theta_C < 90°$, the surface is partially wettable

- $\theta_C > 90°$, the surface is not wettable [58]

The phenomenon of the contact angle can be explained using the relationship of the wettability with the surface tensions of the material. At the

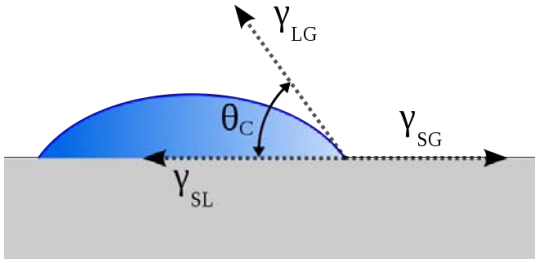

Figure 2.5: Contact angle and surface tensions [59]

equilibrium, all the surface tensions between solid, liquid and vapor phases has to be zero, as showed in the equation (2.1), called Young's equation

$$\gamma_{SG} - \gamma_{SL} - \gamma_{LG} cos(\theta_C) = 0 \tag{2.1}$$

with γ_{SG}, γ_{SL}, γ_{LG} superficial tension between solid and vapor, solid and liquid, and liquid and vapor. The contact angle is given by equation (2.2)

$$cos(\theta_C) = \frac{\gamma_{SG} - \gamma_{SL}}{\gamma_{LG}} \tag{2.2}$$

2.2.4 Cell culture

Culturing cells in an artificial environment is one of the major tools used in molecular and cellular biology, capable to provide models systems for studying not only the normal physiology and biochemistry of the cells, but also the toxicity of drugs or other compounds on the cells, as well as carcinogenesis and mutagenesis. The advantages of the cell culture techniques are the possibility of expanding the available amount of cells, studying cellular processes and reducing the number of animal experiments.

The term cell culture refers to the removal of cells from an animal or plant, which are maintained alive for more than 24 hours in a favourable artificial environment. Cell cultures can be isolated from primary tissue, and they are called primary cultures. This type of culture has a limited life span; the cells can divide a limited number of times, before losing their ability to proliferate. However, some cell lines can undergo through a process called transformation, spontaneously or chemically induced, and become immortal.

In this way, the cell line has the ability to divide indefinitely and it becomes a continuous cell line.

In vivo, cells are surrounded by tissue fluids, which provide all the essential components and remove metabolic products from the organism. In cell culture, the physico-chemical and physiological environment is given by the growth medium. It provides nutrients, growth factors, hormones, and it regulates pH and osmotic pressure of the culture. The only parameter that the media does not control is the temperature: 37 °C and the humidity are provided by incubators, in which cells are placed during the growth.

The growth of cells in culture goes through different phases. The first one is the quiescent or lag phase, this depends on the cell type, the seeding density, the media components and previous handling. During this phase, the cells start to attach to their substrate, synthesizing enzymes, DNA and proteins. There is only a small increase in the number of cells. In the next phase, the log-phase, cells proliferate exponentially, reaching the highest metabolic activity. The length in time of this phase depends on the cell cycle of the cells. During this phase, cells secrete metabolites and require new nutrients; for this reason, the medium should be refreshed. After the exponential growth, cells enter into a stationary phase, where the growth is greatly reduced or entirely ceased [60].

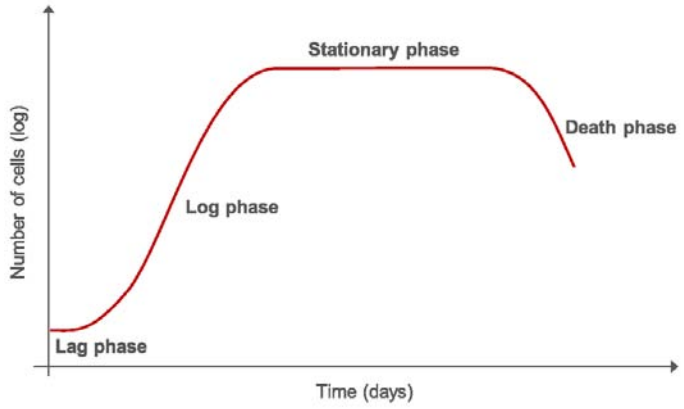

Figure 2.6: Growth pattern of cultured cells [61]

2.2.4.1 Subculturing of cells

When cells reach a semi-confluent state, 70%-80% of the available substrate is covered, the culture has to be divided. This procedure is called subculturing or passaging, and it is referred to the removal of the medium, the detachment of the cells from the substrate by using proteolytic enzymes and

the transfer of cells into a new substrate with fresh medium. If cells are not subcultured, they can lag for a long period and never recover or they might differentiate. Subculturing of cell culture allows to keep cells in an optimal density and to stimulate their proliferation [60].

2.2.4.2 Cryopreservation of cells

If a surplus of cells is available after passaging, it should be frozen. This process is called cryopreservation and it provides the storage of the cells, immersed in complete medium in which is present a cryoprotective agent such as DMSO, in liquid nitrogen. The presence of cryoprotective additives protect the cells from damage during the freezing [60].

2.2.4.3 Thawing of cells

When cells or a new type of cells are needed, it is possible to thaw the frozen cells, stored in liquid nitrogen. The procedure of thawing is stressful for the cells and it has to be a good and quick technique in order to have most of the cells that survived. After thawing, the cells are immerse in medium and store in the incubator [60].

2.2.4.4 Aseptic technique

Maintain an aseptic working area is the main requirement of a cell culture laboratory. For this reason, all the work with cells is performed in a Laminar Air Flow (LAF) cabinet. This sterile environment protect the cell culture from dust and other airborne contaminants, using a constant and unidirectional flow of HEPA-filtered air. In addition, the LAF hood provides a barrier between the culture and the operator. The important elements of an aseptic technique are a sterile working area, good personal hygiene, sterile reagents and media, and sterile handling. The culture hood is large enough to allow one person to work, has the adequate amount of light, and provides a comfortable workstation. The working area has to be maintained clean, uncluttered and with everything on direct sight [60]. Figure 2.7 represents a basic layout of a flow hood. The arrangement is prepared for right-handed workers with the following items: pipettes on the right can be easily reached, media and reagents on rear right for easy pipetting, tube rack on rear middle for additional reagents and waste liquid containers on the rear left. A clear space is present in the center to work on cell culture flasks.

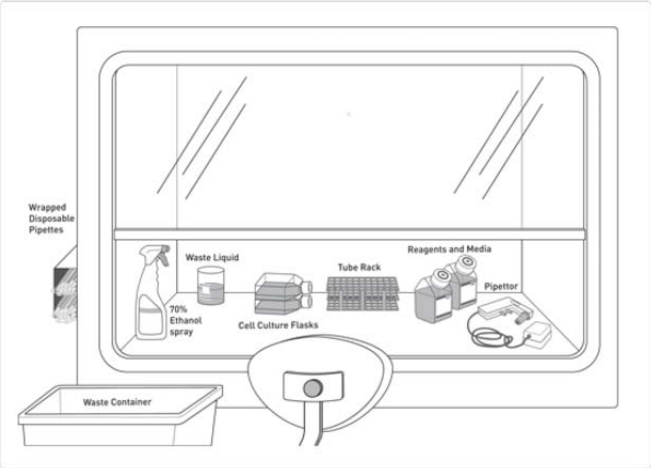

Figure 2.7: Basic layout of a culture hood [60]

2.2.5 Biological fluorenscent stains

After the culture of cells on a substrate, it is possible to quantify the number of cells and their morphology using fluorescence microscopy. In order to see and image the cells, fluorescent dyes are needed. Fluorescent dyes are able to bind to different components of the cell and, after the excitation with light of adequate wavelength, they are able to emit a colour. In this work, the fluorescent stains used are 4',6-Diamidino-2-phenylindole dihydrochloride (DAPI) and phalloidin 488.

DAPI is a DNA-specific probe that increases its fluorescence when it binds to the adenine-thymine (A-T) sequence of the DNA [62], which is contained in the cell nucleus. For this reason, it is used to determine the number of nuclei on the substrate. Its maximum absorption is at wavelength of 358 nm, in the ultraviolet, while its maximum emission is blue light, at wavelength of 461 nm, as shown in Figure 2.8. It has a great photostabil-

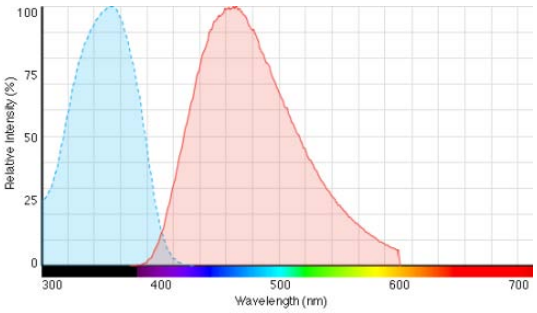

Figure 2.8: Absorption and emission spectrum of DAPI [63]

ity [64]. DAPI can also bind to RNA, but it shows a weaker fluorescence intensity [65].

Phalloidin is a bicycle peptide that belong to the family of toxins called phallotoxins, which are isolated from the *Amanita phalloides*, the death cup mushroom [66]. Phalloidin binds to the F-actin, the filamentous actin, and it allows the investigation of the distribution of the F-actin and consequently of the cytoskeleton of the cells. There are different phalloidin conjugates, with a range of colour choice. The phalloidin stain, used in this thesis, is phalloidin 488 and it has an excitation maximum at wavelength of 493 nm and an emission maximum at wavelength of 519 nm. The fluorescence spectrum is shown in Figure 2.9.

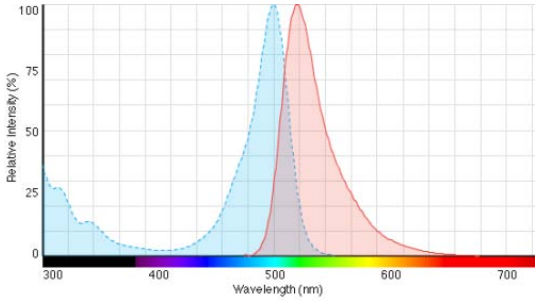

Figure 2.9: Absorption and emission spectrum of Alexa Fluor™488 Phalloidin [67]

In order to use these fluorescent dyes, the cells must be permeabilized and/or fixed before adding them [64]. After the staining, in order to image the cells, it is possible to use a fluorescence microscope, in which are present the appropriate filters to excite and record the fluorescence intensity of the sample.

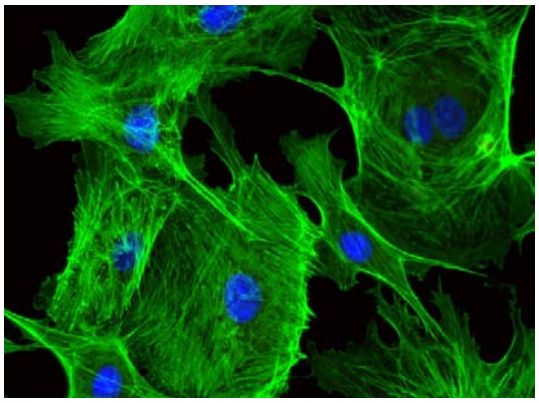

Figure 2.10: Example of bovine pulmonary artery endothelial cells stained with Alexa Fluor® 488 phalloidin and DAPI [68]

Chapter 3

Experimental Part

3.1 Preparation and characterization of the surfaces

3.1.1 Preparation of PCL films

In this work, the polymer used as surface is PCL. To start the project, 2D films were made using a hot press (Specac, Manual Hydraulic Press), in Figure 3.1.

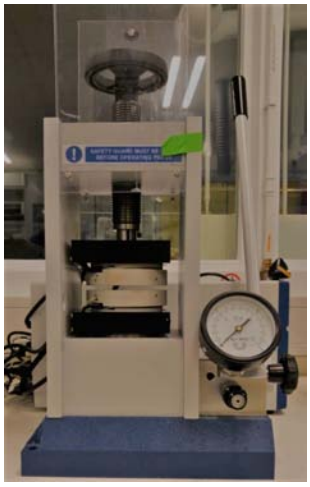

Figure 3.1: Hot press

After opening the water valve and turning on the device, the temperature was set at 95°C, higher than the melting temperature of the PCL (around $60_{\circ}$. Then, the following sandwich was prepared:

- slice of rubber, wrapped with aluminium foil
- silicon wafer
- mold, with 9 circles
- 3 pellets, weighing about 105 mg, of PCL in each circle
- silicon wafer upside down
- slice of rubber, wrapped with aluminium foil.

When the temperature reached 95°C, the sandwich was inserted between the hot plates for 5 minutes to melt. Then, a pressure was applied until there was no space between the silicon wafers and the mold, waiting another 10 minutes. Next, the temperature was decreased to 55°C. After that, the sandwich was demounted and the discs were punched out using a puncher of 15 mm, obtaining PCL films of diameter of 15 mm and thickness of 0.11 mm, showed in Figure 3.2.

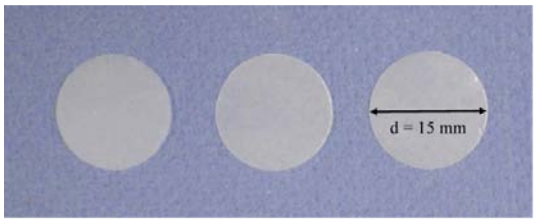

Figure 3.2: PCL films

3.1.2 Characterization of PCL films

PCL films were characterized with FT-IR, GPC and contact angle. These films were used as a control for the modified films and the results obtained from the analysis were used as a reference.

3.1.2.1 FT-IR

FT-IR spectra of a PCL and PCL-modified films were measured with ATR-FTIR Spectrometer (Thermo-Fisher, Nicolet™iS™50 FT-IR Spectrometer), and visualized using OMNIC software. Data were collected between 400-4000 cm^{-1}, at 4 cm^{-1} resolution with 32 scans.

In Figure 3.3, FT-IR spectrum of PCL film is showed, in which it is possible to see the typical peaks of PCL: asymmetric CH_2 stretching at 2944 cm^{-1}, symmetric CH_2 at 2864 cm^{-1}, carbonyl (C=O) stretching at 1720 cm^{-1} and C-O stretching at 1159 cm^{-1}.

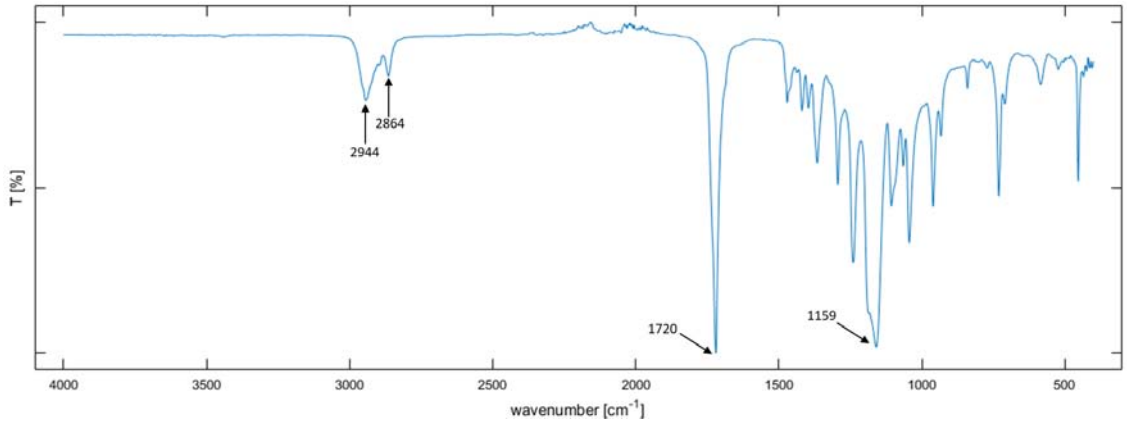

Figure 3.3: FT-IR spectrum of PCL film

3.1.2.2 Contact angle

The contact angle of PCL film was measured using a drop of 6 μl of distilled water. The measurement were repeated 3 times in different parts of the same film. The angle was obtained from an image showed in Figure 3.4, using the software of drop shape analysis (DSA4). The result of the measurement is $\theta_{PCL} = 72.7° \pm 2.09$.

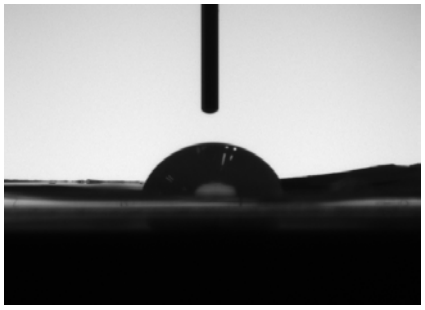

Figure 3.4: Contact angle of PCL film

3.1.2.3 GPC

After the analysis on the PCL film, a small piece of it was cut and dissolved in DMF 0.1% LiBr: 2 mg of polymer were dissolved in 1 mL of DMF 0.1% LiBr. After the dissolution of PCL, the solution was filtered using a PTFE filter of 0.2 μm, and placed in a glass vial, which was inserted in the GPC (Shimadzu, Prominence-i GPC System) for the measurement. The chromatogram obtained at the end of the measurement is showed in Figure 3.5. In Table 3.1, the molecular weight averages.

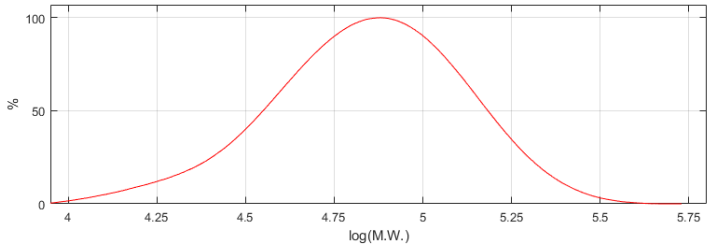

Figure 3.5: GPC chromatogram of PCL film

Table 3.1: Values from GPC

M_n	M_W	PDI
53567	79877	1.49

3.1.3 Aminolysis of PCL films

The first modification of PCL surfaces was aminolysis. In this work, this reaction occurs between the polyester, PCL, and diamine, 1,6-hexanediamine. Aminolysis involves the cleavage of ester bonds and simultaneous formation of amide bonds, NH_2 and OH groups [69]; in particular, one amino group (NH_2) of the diamine reacts with the -COO- group of PCL to form a covalent bond, -CONH-, while the other amino group is free and unreacted [70], as showed in the schemes of Figure 3.6. With the introduction of NH_2 groups on the surface, through the aminolysis reaction, it is possible to increase the hydrophilicity of the surfaces and consequently create a more adequate environment for the cells.

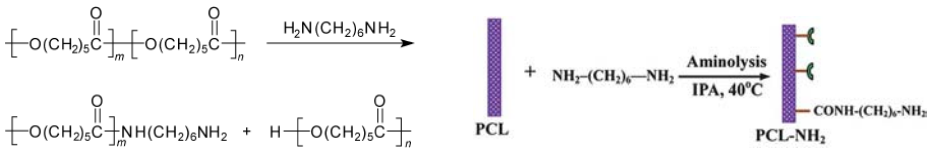

Figure 3.6: Schemes of aminolysis between PCL and 1,6-hexanediamine [71, 72]

PCL films were immersed in 1 mL of a solution of 1,6-hexanediamine/2--propanol with 10 wt% of 1,6-hexanediamine at 37°C (HeratermTM Oven, Thermo-Fisher) for

- 1h
- 4h

Then, the films were rinsed for 1h with deionized water at room temperature, to remove the free 1,6-hexanediamine, and dried overnight [70].

3.1.4 Characterization of aminolysed films

After the aminolysis, the samples were analyzed with FT-IR, GPC and contact angle. In addition, to check the presence of NH_2 groups on the surfaces, a ninhydrin test was performed.

3.1.4.1 Ninhydrin test

Ninhydrin assay is a colorimetric test used for the detection of amino groups on the PCL surface, and consequently the effectiveness of aminolysis reaction [35].

Ninhydrin is a powdered chemical compound of yellow colour, which can reacts with free amino groups, producing a purple colour, called Ruhemann's purple. It was discovered by Siegfried Ruhemann in 1911, who observed the reaction of ninhydrin with α-amino acids [73]. In fact, the detection of amino groups allows using ninhydrin to test the presence of amino acids, peptides and proteins. A scheme of the reaction with an amino acid is showed in Figure 3.7.

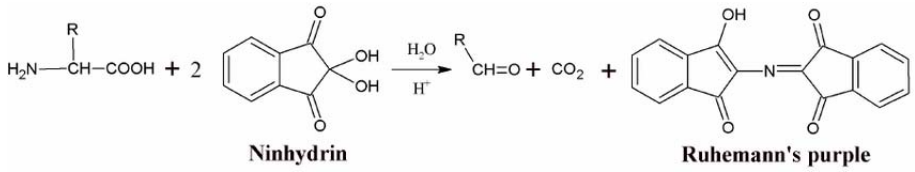

Figure 3.7: Scheme of ninhydrin reaction [74]

In this work, the protocol of ninhydrin assay is the following [75]: first, aminolysed films were cut in small pieces of 8 mm of diameter, and each film was dissolved in 150 μL of 1,4-dioxane. The same amount of 1 mol/L ninhydrin/ethanol solution was added. The obtained solutions were heated at 80°C for 15 minutes and then cooled in ice bath. The solutions were transferred on a 96-well plate and the absorbance between 450 nm and 650 nm were measured using a plate reader (BMG Labtech, CLARIOstar® High Performance Microplate Reader). A calibration curve was obtained using known concentration of 1,6-hexanediamine in 2-propanol/1,4-dioxane with the addition of ninhydrin/ethanol solution. The absorbance spectrum of the solutions of different known concentration of 1,6-hexanediamine, between 450 nm and 650 nm, is showed in Figure 3.8. After the analysis, the absorbance of the samples had a maximum peak at 492 nm and, for this reason, the calibration curve was obtained from the absorbance spectra at a wavelength of 492 nm. The calibration curve relates the absorbance with

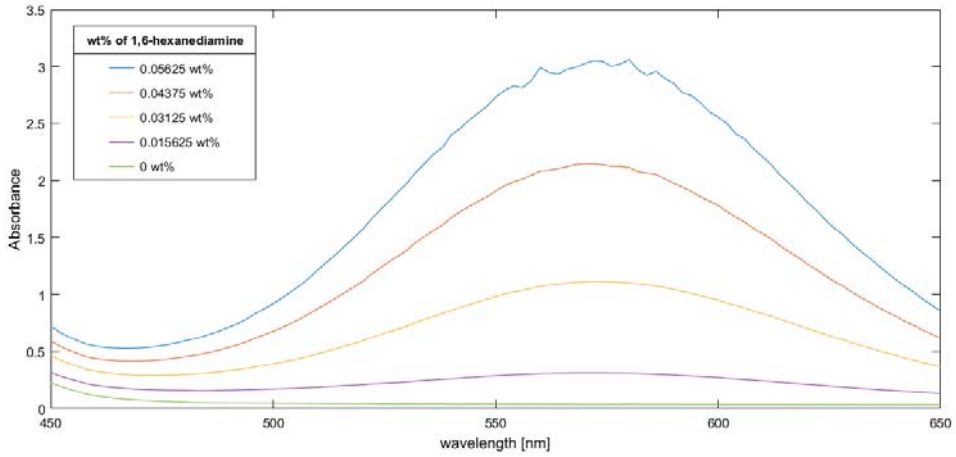

Figure 3.8: Spectra of different wt% of 1,6-hexanediamine

the NH_2 concentration in the solution. From the calibration curve, it is possible to calculate the amino groups concentration in the aminolysed samples. The calibration curve was obtained from the previous spectra using Basic Fitting tool of MATLAB® (R2017b), choosing linear fitting; the software provided the equation of the calibration curve and the calculation of R^2, the coefficient of determination.

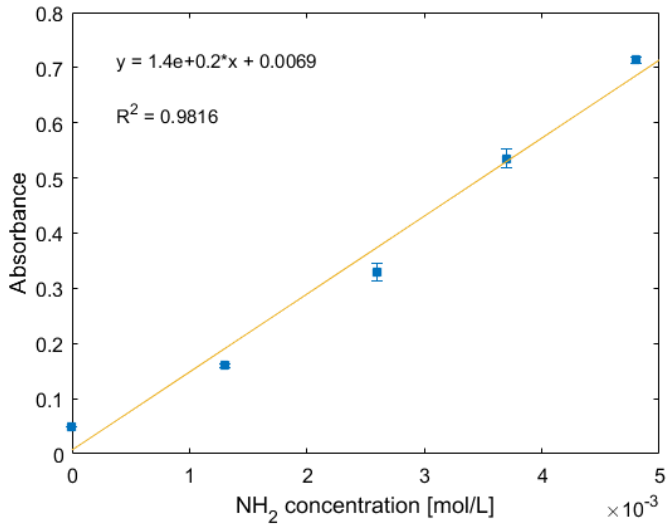

Figure 3.9: Calibration curve of reaction ninhydrin-NH_2

3.2 Cell culture

MG 63 ostesarcoma cells were thawed and cultured in flasks. The medium used for the culture was α-MEM without nucleosides, to which 10% of volume of FBS was added. The medium was refreshed every other day until the cells reached 70%-80% of confluency and then trypsinized to replate or to cryopreserve.

3.2.1 Trypsinization

Trypsin is a serine protease, found in digestive system of many vertebrates. It hydrolyses proteins: when trypsin is added to a cell culture, it cleaves the peptide bonds in the proteins that enables the adhesion of cells to the flasks and between them. The breakdown of the proteins allows the detachment of the cells from the substrate, but at the same time, trypsin breaks down also the other proteins of cell membrane and that can affects the functioning of the cells [76]. For this reason, trypsin has to be inactivate to avoid destructive effects on the cell culture. Trypsinization procedure for a T225 flask is the following:

- Remove the medium from the flask
- Washing step: (x2 times)
  - Add 4 mL of PBS in the flask
  - Remove the PBS
- Trypsin step:
  - Add 4 mL of trypsin in the flask
  - Incubate the flask at 37°C for 4 minutes
  - Check the cells with the microscope and tap if the cells do not get loose
- Deactivation step:
  - Add 8 mL of medium directly on the bottom of the flask to collect all the cells
- Transfer all the medium with cells to a plastic tube

3.2.1.1 Cell counting

Cells are seeded on a surface using a certain density of cells/cm^2. Trypan blue and a Neubauer chamber are used to count the collected cells; in this way it is possible to calculate the number of cells that are needed for the seeding.

Trypan blue is a blue acid dye, containing two azo chromophores [77]. It is employed in dye exclusion tests in order to determine the number of viable cells in suspension [78]. This is possible because live cells that have intact membrane excludes trypan blue, which can permeate cell membrane of dead cells. For this reason, looking at the cells in the microscope, the live ones look clear, whereas the dead one are blue. The Neubauer chamber provides a scheme and a formula to determine the number of cells. The layout of the chamber is showed in the Figure 3.10: the cells are counted in the 5 highlighted squared.

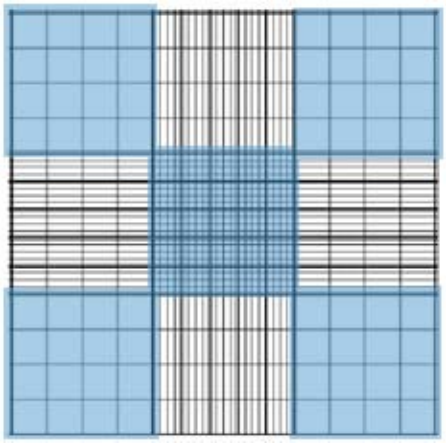

Figure 3.10: Layout of Neubauer chamber [79]

The formula is the following:

$$Concentration\,(cells/mL) = 2 \times \frac{number\,of\,counted\,cells}{number\,of\,squares} \times 10000$$

and it keeps into account the dilution of the cells with the trypan blue.

The counting procedure, used in the laboratory, was performed using 20 μL of trypan blue to which 20 μL of cells in medium were added. Then, 10 μL of this solution was put in the chamber and the cells are counted using the microscope.

3.2.2 Cell seeding

After the preparation and modification of the surfaces, PCL and aminolysed films were seeded with MG 63 osteosarcoma cells, at passage P 93.

For each time point, samples used for cell seeding were triplets of films of the following conditions

- PCL
- PCL Aminolysis 1 h
- PCL Aminolysis 4 h

Prior to cell seeding, the samples were sterilized, immersing them in ethanol 70% for 10 minutes and drying them on autoclaved paper filter. After the sterilization, the samples were placed in 24-well plates, using O-rings to keep them on the bottom of the well. The O-rings were sterilized as well using the same procedure. The samples were covered with 1 mL of α-MEM + Glutamax/10% FBS + 1% of Pen/Strep and incubated at 37°C for 10 minutes, before adding the cells.

The films had a diameter of 15 mm and an area of A=1.76 cm^2. The cell density used for the seeding was 5000 cells/cm^2, meaning around 9000 cells per film. After the counting, cells were added randomly to the medium in each samples. Cells seeded on films were analysed at

- Day 1
- Day 7

3.3 Biological characterization

In order to observe the cells and be able to analyse them, two different stains were used: DAPI and phalloidin 488. Prior to staining, the cells were fixed on the samples: in this way, the cells are not alive, but they maintain their shape.

3.3.1 Fixation of cells

After 1 day and 7 days, the cells were fixed on the films, with the following procedure:

- Remove 900 uL of medium from each well
- Add 100 uL of 8% PFA solution to each well

- Place the well-plate at 4°C for 20 minutes

Leaving 100 uL of medium, instead of removing the entire medium, to prevent from damaging the samples, giving a final concentration of PFA solution of 4%.
After the incubation in the refrigerator

- Remove the fixation solution from each well
- Add 1 mL of PBS to each well
- Repeat PBS wash 3 times
- Leave 1 mL of PBS in each well to store the samples in the refrigerator

3.3.2 DAPI and phalloidin staining

Prior to staining, the cells need to be permeabilize, in order to allow the staining to pass through the cell membrane. The procedure to permeabilize the cells is described here:

- Replace PBS in each well with 300 uL of 0.1% Triton® X-100 in PBS
- Incubate the samples for 15 minutes at room temperature
- Remove the permeabilization solution from each well
- Wash 3 times with 500 uL of PBS
- Leave 500 uL of PBS to maintain the samples wet

After the permeabilization step, it is possible to start immediately with the staining: first, the phalloidin staining, then the DAPI staining.
The solution for the phalloidin staining was prepared as following:

- 5 uL of methanolic stock solution into 200 uL of 1% BSA in PBS

and the procedure of the phalloidin staining is described below:

- Replace PBS with 300 uL of staining solution per well
- Incubate the samples for 20 minutes at room temperature in the dark
- Remove the staining solution from each well
- Wash the samples with 500 uL of PBS
- Repeat PBS wash for 3 times

Lastly, the solution for the DAPI staining was prepared:

- 0.1 ug of DAPI per 1 mL of PBS

and after the last PBS wash of phalloidin step, the DAPI solution is used as following:

- Replace PBS with 300 uL of DAPI solution per well
- Incubate the samples for 15 minutes at room temperature in the dark
- Remove the staining solution from each well
- Wash the samples with 500 uL of PBS
- Repeat PBS wash for 3 times
- Leave 500 uL per well for the imaging

3.3.3 Microscope images

Triplicates of the samples were imaged using a fluorescence microscope (Nikon, Inverted Microscope Eclipse Ti-S), with different excitation and emission filters, matching the wavelengths of phalloidin 488 and DAPI, as described in section 2.2.5. Each film was imaged 3 times, in different parts of the surface. The images from the two channels were merged with ImageJ [80]. The counting of the number of nuclei present in each image was performed using CellProfiler [81], in particular the analysis module of identification of primary objects.

3.4 Preparation and characterization of the surfaces

The main purpose of this project is the functionalization of the PCL surface with a RGD peptide, through the coupling with polymer brushes. The first step, to achieve the ultimate goal, is the preparation of the PCL surface, with an element that allows the coupling with the brushes: for this reason, PCL is functionalized with maleimide. This compound can link the PNIPAM brushes, containing an aldehyde group. This functional group is needed because it can couple with the specific amino-oxy group, present on the RGD peptide. A schematic representation of the final structure of the surface is given in Figure 3.11.

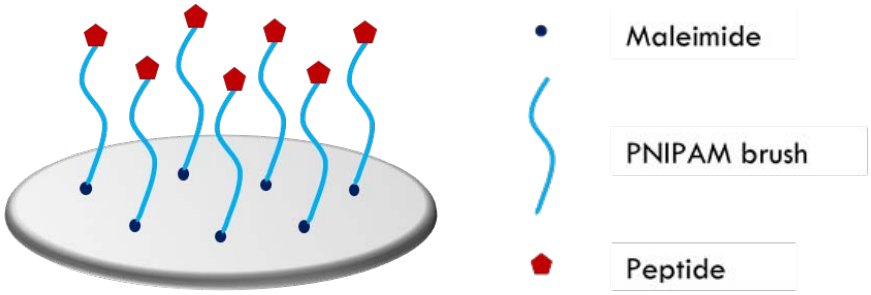

Figure 3.11: Scheme of PCL-maleimide-PNIPAM-peptide structure

3.4.1 PCLM surfaces

Maleimide is a chemical compound of structural formula in Figure 3.12.

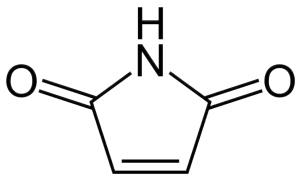

Figure 3.12: Structural formula of maleimide [82]

The functional group of maleimide can be used to create different macromolecular architectures, through the coupling reaction between maleimide and thiol group [83]. PCL was functionalized with maleimide, obtaining PCL-maleimide (PCLM), of molecular weight between 7000 g/mol from NMR and 15000 g/mol from GPC. In order to create films with maleimide on the surface, the compound of PCLM was mixed with PCL M_n=45,000, in different percentages:

- 1% of PCLM
- 10% of PCLM

The mix of these percentages of PCLM with PCL was done using an extruder (Thermo Scientific HAAKE MiniCTW), in Figure 3.13. The temperature was set on 63°C, the speed of the screws at 100 rpm, and the materials were inserted and left to mix for 10 minutes. Then, the temperature was decrease at 55°C: after reaching it, the screws' speed was decrease to 5/10 rpm and the material was extruded, obtaining fibers of material.

The procedure of each percentage of PCLM was repeated two times. The fibers from the second extrusion were cut in small pieces and used to make

Figure 3.13: Thermo Scientific HAAKE MiniCTW [84]

films, as described for the PCL films in section 3.1.1. The different steps are showed in Figure 3.14.

Figure 3.14: Steps from extruded PCL-PCLM fibers to films

3.4.1.1 BSA-FITC

Albumin-fluorescein isothiocyanate conjugate (BSA-FITC) was used to check the presence of maleimide on the surface of the films. This conjugate is composed of a protein, bovine albumin serum (BSA), and a labelling agent, fluorescein isothiocyanate (FITC), which bind the proteins through the amino group of a residue [85]. FITC is a popular fluorescent probe that has its excitation at wavelength of 495 nm and its emission at wavelength of 519 nm, giving a green colour. The conjugation of the labelled-protein and the maleimide occurs through the bond between maleimide and sulfhydryl group on the protein, as showed in Figure 3.15.

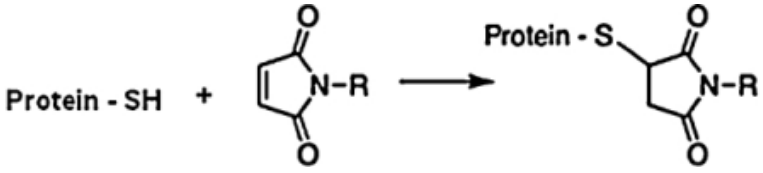

Figure 3.15: Reaction scheme bteween maleimide and protein [86]

To test the samples, a solution of PB buffer at pH=7 with a concentration of 1 mg/mL of BSA-FITC was prepared. 2 samples of the following conditions

- PCL
- 1% PCLM
- 10% PCLM

were place in a 24 well-plate and immersed in 600 μL of BSA-FITC/PB buffer solution for 24 hours at room temperature, covered with aluminium foil. At the same time, 1 sample of each condition was immersed in only PB buffer, as control. After the determined time, all the samples were washed 3 times with PB buffer. The analysis of the samples was performed using the plate reader (BMG Labtech, CLARIOstar® High Performance Microplate Reader) and the microscope (Nikon, Inverted Microscope Eclipse Ti-S) .

3.5 Introduction of polymer brushes

After the preparation of the PCLM surfaces and the test of the presence of maleimide on the surfaces, polymer brushes made of PNIPAM were prepared.

3.5.1 Preparation of the polymer brushes

The polymer used for the brushes is PNIPAM. It was prepared by my daily supervisor, from NIPAM with RAFT polymerization.

3.5.1.1 RAFT polymerization

The three principal mechanisms employed for reversible-deactivation radical polymerization are:

- Polymerization with reversible termination coupling
- Radical polymerization with reversible termination by ligand transfer to a metal complex, usually called atom-transfer radical-polymerization (ATRP)
- Free-radical polymerization with reversible chain transfer or RAFT polymerization [87]

Reversible addition-fragmentation chain transfer (RAFT) was developed at CSIRO in the 1990s and it is a robust and versatile method to control radical polymerization [88]. The mechanism of this controlled polymerization involves a chain growth that is initiated by a free radical initiator, such as AIBN, and mediated by a dithioester chain transfer agent, usually called

RAFT agent. The transfer of radical between the growing chains gives a good control of the polymerization, while the presence of the dithioester moiety gives a good living character to the reaction [44]. A scheme of the overall RAFT process is shown in Figure 3.16, where Z is the activating group and R the free-radical leaving group [88].

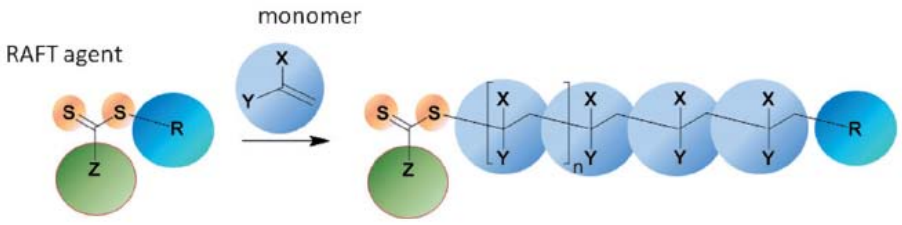

Figure 3.16: RAFT process [88]

The success of the RAFT polymerization is given by the effectiveness of the RAFT agent and consequently, by the choice of Z and R groups. Selecting the appropriate RAFT agent and the reaction conditions, RAFT polymerization is applicable to a wide range of monomers, obtaining controlled molecular weight polymers with very narrow polydispersity [87]. This provides the ability to synthetize well-defined homo-, gradient, diblock, triblock and star polymers, and more complex architecture, including microgels and polymer brushes, which are not synthetize with other methods [88].

In this work, RAFT polymerization was used to synthetize the PNIPAM brushes. These were obtained from NIPAM, using AIBN as initiator, 1,4.dioxane as solvent and the following RAFT agent, prepared by Dr. Huey Wen Ooi, based on Jackson et al. [89]:

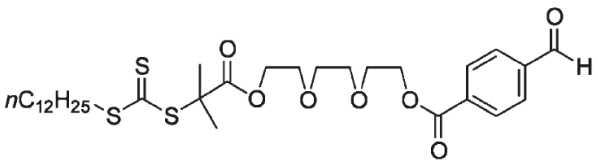

Figure 3.17: RAFT agent [89]

The temperature was set at 60°C and the reaction was performed for 6 hours.

3.5.2 Addition of PNIPAM brushes

In order to add the polymer brushes to PCL and PCLM samples, a solution of PNIPAM brushes was prepared and each film was immersed in 600 μL of

it. The components for the preparation of the solution of PNIPAM brushes were:

- PNIPAM
- TCEP
- 1,4-dioxane
- Ethylenediamine
- Diethyl ether
- Nitrogen

PNIPAM M_n=23,000 was weighted for a final concentration of 10 mg/mL and a crystal of TCEP was added. The polymer was dissolved in 1,4-dioxane and the solution was degassed using nitrogen for 15 minutes. Then, 1 M of ethylenediamine was added to the solution, followed by degas for other 15 minutes. This step was needed to remove the RAFT agent from PNIPAM and it was demonstrated by the changing in colour, from yellow to transparent, of the solution. After that, the solution was leaving to stir, while diethyl ether was degassed with nitrogen for 15 minutes. At the end, the solution was precipitate in diethyl ether, which is non solvent, collecting the polymer at the bottom of the tube. PNIPAM with diethyl ether was centrifuge (Centrifuge 5430 R, Eppendorf) at 4°, 5000 rpm for 10 minutes. After the centrifugation, the diethyl ether was removed and the PNIPAM was let it dry. The final solution used for the samples was made of the obtained PNIPAM, dissolved in PB buffer, at pH=7. The sample were immersed in 600 μL of this solution for two days and then washed for 3 times with PB buffer.

3.5.2.1 Alkoxyamine-PEG4-Biotin

To test the presence of the brushes on the surface of the films, a particular dye was used: Alkoxyamine-PEG4-Biotin, of structure showed in Figure 3.18. This dye contains an amino-oxy group, the same functional group present in the peptide, and it couples with the aldehyde group, present in the PNIPAM brushes. Details on this reaction are given in section 3.6.

Alkoxyamine-PEG4-Biotin was dissolved in DMSO with a concentration of 250 mM and then, it was added to PB buffer pH=7, with a concentration of 0.2 mg/mL. PCL and PCLM films with added PNIPAM brushes were immersed in 600 μL of this solution for 24 hours. The samples were analysed

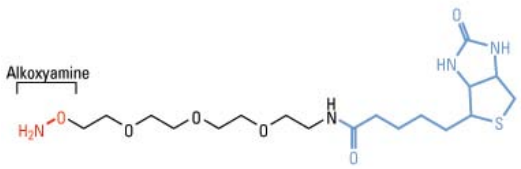

Figure 3.18: Alkoxyamine-PEG4-Biotin [90]

with the plate reader (BMG Labtech, CLARIOstar® High Performance Microplate Reader) and the microscope (Nikon, Inverted Microscope Eclipse Ti-S). The wavelength used for analysing these samples was checked using the PDA detector of the GPC (Shimadzu, Prominence-i GPC System). The result of the measurement is shown in Figure 3.19.

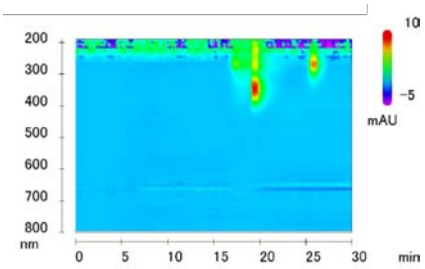

Figure 3.19: Result of PDA detector of GPC for Alkoxyamine-PEG4-Biotin

The signal of the dye showed around 20 minutes, at wavelength between 300 nm and 400 nm. The other signal, after 25 minutes, it was given by the solvent.

3.6 Introduction of the peptide

After the addition of the PNIPAM brushes to the PCL and PCLM films, RGD peptide was added to the films. The coupling between the brushes and the peptide is specific: in the PNIPAM brushes is present an aldehyde group, while the peptide has an amino-oxy group. The reaction between these two functional groups is shown in Figure 3.20.

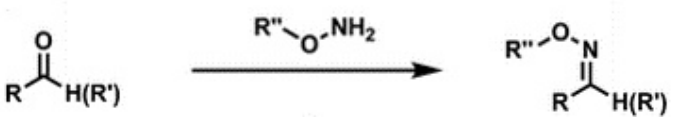

Figure 3.20: Aldehyde - amino-oxy reaction [91]

3.6.1 Amino-oxy - aldehyde small molecule test

Amino-oxy - aldehyde small molecule test was used to analyse the coupling between these two functional groups and estimate the concentration of compounds, containing amino-oxy and aldehyde groups, to obtain the higher coupling between them.

In this work, the small molecule test was carried out using the following compounds containing the functional groups of interest:

- 4-Amyloxybenzaldehyde
- Carboxymethoxylamine

These were dissolved in PB buffer at pH=7 in different mole ratios:

- 1 : 1
- 1 : 2
- 2 : 1
- 1 : 4
- 4 : 1

and left to shake for 24 hours.

To verify the coupling, a dye that reacts in presence of aldehydes was used. The name of this substance is 4-amino-3-hydrazino-5-mercapto-1,2,4--triazole, but it is usually called Purpald®, to give an indication of its application. It turns purple when aldehydes are present. The scheme of the reaction is shown in Figure 3.21.

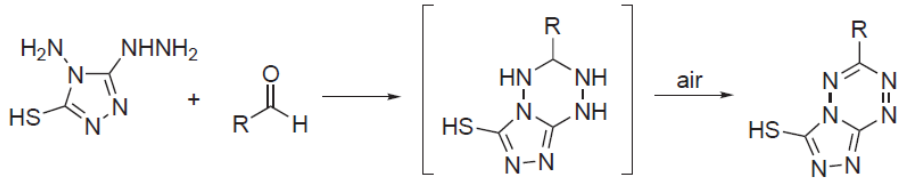

Figure 3.21: Reaction between Purpald® and aldehydes [92]

The solution for the detection of the aldehydes was prepared dissolving Purpald® in NaOH with a concentration of 5 mg/mL. Then, 10 μL of each solution of different molar ratio was added to 500 μL of Purpald®/NaOH solution. When the purple colour showed in the solutions, around 30 minutes after the mixing, t he solutions were transferred on a 96-well plate and the absorbance between 450 nm and 650 nm was measured with the plate reader (BMG Labtech, CLARIOstar® High Performance Microplate Reader).

3.6.2 Preparation of RGD peptide

The peptide Aoa7GRGDSP (sequence: NH_2-O-CH_2-CO-7-aminoheptanoic acid-Gly-Arg-Gly-Asp-Ser-Pro-NH_2) was synthesized on Rink Amide MBHA resin (0.60 mmol/g) using Fmoc chemistry by a Syro I synthesizer (Multi-syntech, Witten, Germany). The side chain protecting groups were: OtBu, Asp; tBu, Ser; Pbf, Arg. The couplings were double for the first insertion, then single (5 equivalents of Fmoc-amino acid, 5 eq. HBTU, 5 eq. HOBt and 10 eq. DIEA, for the last coupling 10 eq. of 2,4,6-Collidine was used instead of DIEA). The peptide was deblocked from the resin and deprotected from side chain protecting groups using the mixture 1,9 mL TFA, 0.05 mL TES, 0.05 mL H_2O, for 1.5 h. The identity and homogeneity of crude peptide was ascertained by mass and RP-HPLC analyses.

3.6.3 Addition of RGD peptide

The solution containing the peptide was prepared dissolving 0.2 mg/mL of Aoa7GRGDSP peptide in PB buffer, at pH=7. Before the immersion of the samples in this solution, all the PCL/PCLM films + PNIPAM brushes were sterilize in ethanol 70% for 10 minutes and then dried, and the solution was filtered using a 0.2 μm filter. These steps were performed in a cell culture cabinet. Then, the samples were immersed in 600 μL of peptide solution for a week. At the end, the samples were washed 3 times with filtered PB buffer.

3.7 Cell seeding

The following surfaces were prepared:

- PCL, 1% PCLM, 10% PCLM, as controls
- (PCL, 1% PCLM, 10% PCLM) + PNIPAM brushes
- (PCL, 1% PCLM, 10% PCLM) + PNIPAM brushes + RGD peptide

For each time points, triplets of these samples were seeded with MG 63 osteosarcoma cells, at passage P 95. The sterilization of the samples and the preparation of the well-plates were the same as described in section 3.2.2. The only difference is that the samples were not incubated with the medium α-MEM + Glutamax/10% FBS + 1% of Pen/Strep; 1 mL of this was added to each sample immediately before the introduction of the cells. The area of the film was A=1.76 cm^2 and the cell density was 5000 cells/cm^2. Cells seeded on films were analysed at

- Day 1
- Day 3

3.8 Biological characterization

After 1 day and 3 days, the seeded cells were fixed, stained with DAPI and phalloidin 488 and then analysed. The procedures of all these steps were already described in section 3.3.

3.8.1 Microscope images

Triplicates of the samples were imaged using a fluorescence microscope (Nikon, Inverted Microscope Eclipse Ti-S). This time, each film was imaged 5 times, starting from the center of the sample and followed a clockwise rotation. The images from the two channels were merged with ImageJ [80] and a representative image is shown as result. The counting of the number of nuclei present in each image was performed using CellProfiler [81], in particular the analysis module of identification of primary objects.

3.9 Optimization of introduction of brushes and peptide

The last section of this work refers to the optimization of the following steps:

- Addition of the PNIPAM brushes
- Addition of the RGD peptide

These procedures were repeated with new films in presence of a catalyst, in order to increase the rate of the reactions and to have more effectiveness of the coupling between maleimide, brushes and peptide.
In addition, another percentage of PCL-maleimide was introduced: PCL was mixed with

- 20% of PCLM

This higher percentage of maleimide was added to show greater differences between PCLM samples.

3.9.1 Optimization of addition of polymer brushes

PNIPAM for the brushes was prepared in the same way as described in section 3.5.2. Then, 10 mg/mL of PNIPAM was dissolved in a solution of:

- PB buffer, pH=7
- TEA, a catalyst

The concentration of the catalyst was 1% of the volume of the final solution. The samples were immersed in 600 μL of this solution overnight. After that, the films were washed 3 times with PB buffer.

To test the coupling, the samples were analyzed using FT-IR and contact angle. In addition, Alkoxyamine-PEG4-Biotin was used, following the procedure of section 3.5.2.1. The only differences were the lenght of the reaction and the prepared solution. The samples were immersed overnight in 600 μL of a solution made of

- PB buffer, pH=7
- 0.2 mg/mL of Alkoxyamine-PEG4-Biotin
- 10 mM of *m*-phenylenediamine, a catalyst

3.9.2 Optimization of addition of peptide

In the same way, the solution for the peptide was made of

- PB buffer, pH=7
- 0.2 mg/mL of RGD peptide
- 10 mM of *m*-phenylenediamine, a catalyst

Then, the solution was filtered using a 0.2 μm filter and 600 μL of it were added to the, already sterile, PCL/PCLM films + brushes. The samples were immersed in the solution for 2 days, followed by 3 washes with PB buffer.

3.9.3 Cell seeding

The following surfaces were prepared

- PCL, 1% PCLM, 10% PCLM, 20% PCLM as controls
- (PCL, 1% PCLM, 10% PCLM, 20% PCLM) + PNIPAM brushes

- (PCL, 1% PCLM, 10% PCLM, 20% PCLM) + PNIPAM brushes + RGD peptide

For each time point, triplets of these samples were seeded with MG 63 osteosarcoma cells, at passage P 97. The sterilization of the samples and the preparation of the well-plates were the same as described in section 3.7. The area of the film was A=1.76 cm^2 and the cell density was 5000 cells/cm^2. Cells seeded on films were analyzed at

- Day 1
- Day 3

3.9.4 Biological characterization

After 1 day and 3 days, the seeded cells were fixed, stained with DAPI and phalloidin 488 and then analyzed. The procedures of all these steps were already described in section 3.3.

3.9.5 Microscope images

Triplicates of the samples were imaged using a fluorescence microscope (Nikon, Inverted Microscope Eclipse Ti-S) and each film was imaged 5 times, starting from the center of the sample and followed a clockwise rotation, as reported for the previous experiment. The images from the two channels were merged with ImageJ [80] and a representative image is shown as result. The counting of the number of nuclei present in each image was performed using CellProfiler [81], in particular the analysis module of identification of primary objects.

3.9.6 Statistical analysis

The results of the counting are expressed as mean ± standard deviation (SD) of the triplicates of films for each condition. If it was not possible to obtain all the images from a film, the calculation of the mean was adjust accordingly and taking into account the presence of less information. The results were calculated in Excel. Statistics were performed using ANOVA test in GraphPad Prism 7. Statistical significance between the modified films and the respective controls was expressed as p-value ($* \ p<0.05$)

Chapter 4

Results and Discussion

In this chapter, the results and the discussions about the analysis, described in the experimental section, will be presented. The principal outcomes of the project are represented by the preparation of different surfaces and the immobilization of different compounds on them. Furthermore, the seeding of cells on these surfaces are shown through the use of biological staining, followed by the counting of the number of cells present on the different films and the comparison between them.

4.1 Aminolysed films

First modification of PCL surfaces was aminolysis. After that, the samples that were analysed using FT-IR and the ninhydrin test were the following:

- PCL
- PCL-NH_2 1h
- PCL-NH_2 4h

Where PCL-NH_2 indicates the samples after aminolysis, namely after the introduction of amino groups, followed by the duration of the reaction.

4.1.1 FT-IR

First, the samples listed above were analysed with FT-IR. The spectra obtained from the measurements are shown in Figure 4.1.

Beside the typical peaks of PCL, described in section 3.1.2.1, three additional peaks are present in the spectra of aminolysed films:

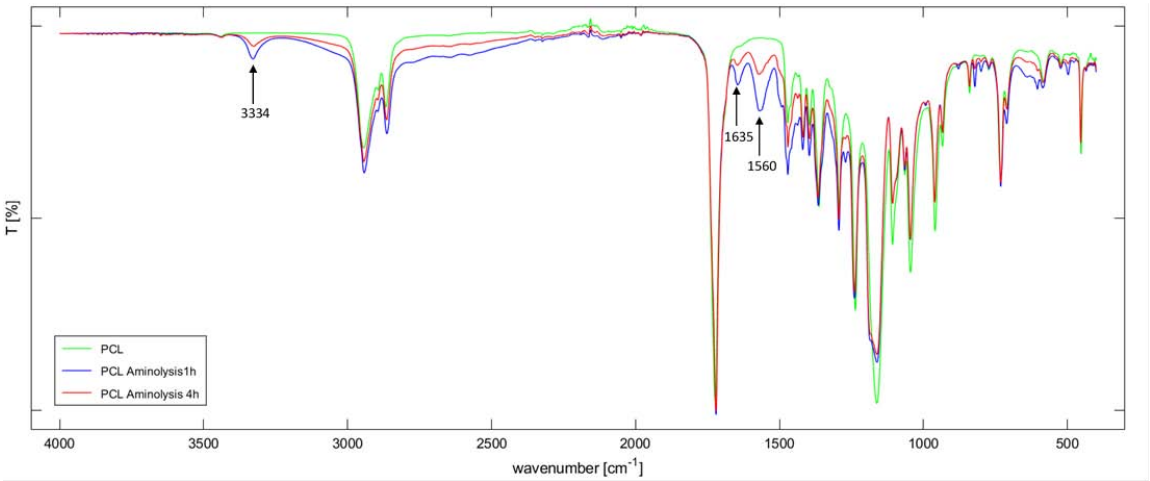

Figure 4.1: FT-IR spectrum of PCL/PCL-NH_2 films

- at wavelength 3334 cm^{-1} attributable to N-H stretching
- at wavelength 1635 cm^{-1} attributable to C=O bending
- at wavelength 1560 cm^{-1} attributable to N-H bending [72]

The presence of these three additional peaks in the aminolysed samples evidences the immobilization of the amino group on the surface [93, 72]. All the aminolysed samples show the peaks, but the sample PCL-NH2 1h has a higher signal in the IR regions of interest, showing that the increase of the time of the aminolysis reaction does not necessarily lead to an increase of the amino groups present on the surface.

4.1.2 Ninhydrin test

After the FT-IR measurements, the aminolysed samples were tested using the ninhydrin, as explained in section 3.1.4.1. The result of the absorbance of the samples is shown in Figure 4.2.

In literature [70, 35, 94, 95, 96], the absorbance of the aminolysed samples is usually analysed at wavelength between 515 nm and 570 nm, while the samples analysed in this work show shifted peaks, with a maximum around 492 nm. Furthermore, the absorbance values are very low, because, from a visual inspection, the samples did not show a very strong purple colour. This result may be due to the incomplete reaction of the ninhydrin with the amino groups, showing the absorbance peaks in a different IR region. However, it was possible to obtain a linear calibration curve at 492 nm, as shown in Figure 3.9, and to calculate the number of NH_2 groups on the surface: 1.96

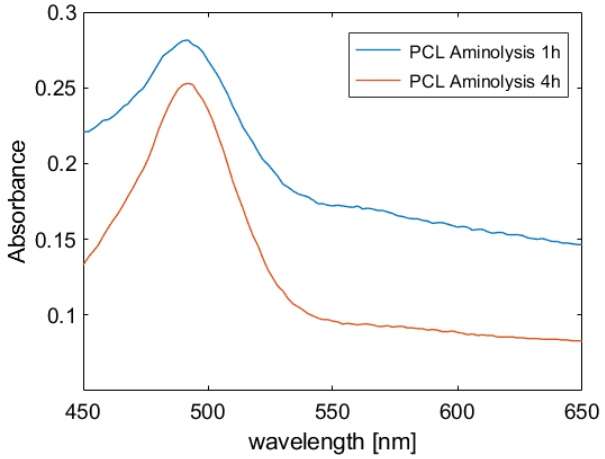

Figure 4.2: Absorbance of PCL-NH_2 films after ninhyderin test

$\times$ 10^{-3} mol/L for the sample PCL-NH_2 1h and 1.75 $\times$ 10^{-3} mol/L for the sample PCL-NH_2 4h. These values of the concentration of NH_2 groups on the surfaces are larger than an order of magnitude compared to the numbers for the same values of absorbance, but measured at different wavelength, found in literature [70]. Even if the reaction of the ninhydrin with the surfaces did not work completely, the absorbance of the PCL-NH_2 1h is higher compared to the absorbance of the sample PCL-NH_2 4h, according to the FT-IR results on the same samples. The value of amino groups was expected to reach a maximum around 1h of exposure to 1,6-hexanediamine, as reported in literature [70, 94, 95]. The reaction with carboxyl of free amino on terminal chain or the degradation of superficial layer may cause the decreasing of amino groups for longer period of aminolysis [70].

After the measurements and tests on the samples, all of them were seeded with MG 63 osteosarcoma cells. The use of the cells allows testing if the aminolysis reaction, with the introduction of polar groups on the surface [69], creates a more appropriate environment for the cells, compared to only PCL surface.

4.2 Biological characterization of aminolysed films

On PCL and PCL-NH_2 surfaces, MG 63 osteosarcoma cells were seeded. The cells on the films were fixed after 1 day and 7 days, stained and then analysed.

The images obtained with the microscope are shown in Figure 4.3 and represent a portion of PCL, PCL-NH_2 1h and PCL-NH_2 4h surfaces after

1 day. The results of counting of nuclei is presented with a graph in Figure 4.5(a).

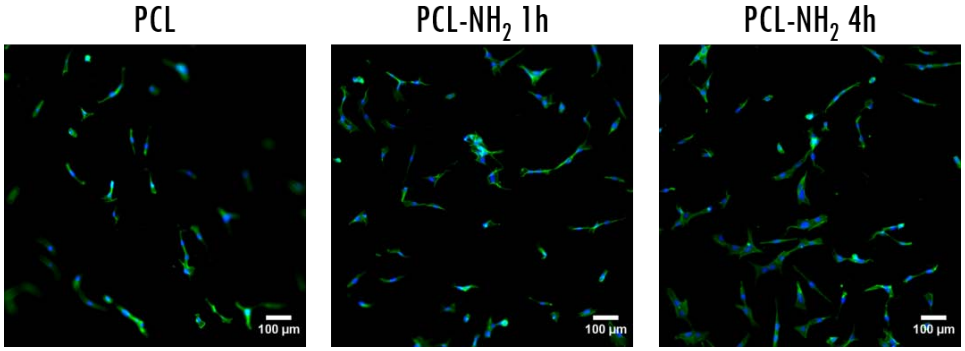

Figure 4.3: Day 1: Phalloidin 488 and DAPI staining of cells on PCL, PCL-NH_2 1h and PCL-NH_2 4h surfaces

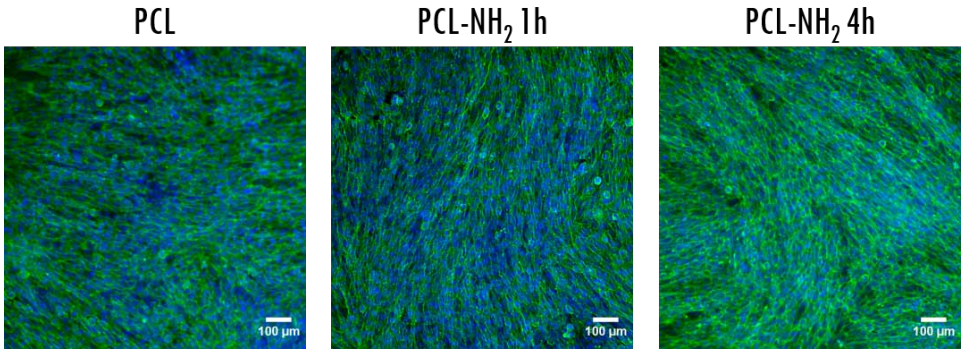

Figure 4.4: Day 7: Phalloidin 488 and DAPI staining of cells on PCL, PCL-NH_2 1h and PCL-NH_2 4h surfaces

From the analysis of the images and the counting, it is possible to notice that the number of cells in the PCL film is lower respect to the PCL-NH_2 samples, whereas there is not an evident difference between the films modified with the aminolysis reaction.

In Figure 4.4, the images of cells on the surfaces after 7 days. In these samples, the number of cells is high, both in PCL and in PCL-NH_2 surfaces, making difficult to obtain a reliable result from the count of cells. Taking into account this observation, the counting reveals that the number of cells on the PCL-NH_2 films is higher compared to the PCL film, but also in this case the difference between the time points of the PCL-NH_2 films is not significant, as shown in the graph in Figure 4.5(b).

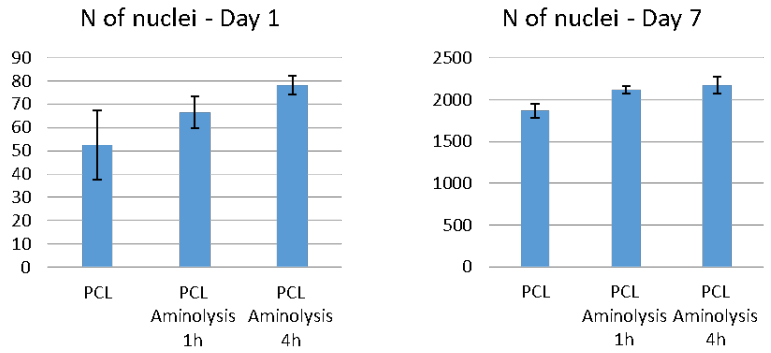

(a) (b)

Figure 4.5: Number of nuclei

The high presence of cells in the PCL films can be due to the incubation with the medium of the surface, before the introduction of the cells. The components of the medium, in particular proteins, can be adsorbed on the surface and attract the cells to adhere. In addition, there is no other space where the cells can go, except the surface. The cells cannot go through the sample.

In conclusion, the presence of NH_2 groups on the surface increases the adhesion of the cells compared to the PCL sample, but the different length in time of the reaction does not show a noticeable difference. From the results of FT-IR and cell seeding, the only sample of PCL-NH_2 1h can be used for further analysis, without needing of samples with a longer time of the aminolysis reaction.

4.3 PCLM surfaces

The surfaces for the functionalization with brushes and with RGD peptide were prepared by mixing PCL with PCL-maleimide in different percentages:

- 1% PCLM
- 10% PCLM

These surface and PCL films were tested with BSA-FITC in order to see if maleimide is present on the surface of the films. The fluorescence of the BSA-FITC on the surfaces was tested with the plate reader and in order to show the emission at 519 nm of BSA-FITC, the surface were imaged with the microscope. The obtained images were shown in the Figure 4.6

Figure 4.6: Fluorescence images of PCL, 1% PCLM and 10% PCLM

The first row represents the samples immersed in PB buffer and the second row shows the samples after the immersion in a solution of BSA-FITC. From left to right, the samples are PCL, 1% PCLM and 10% PCLM. In the following Table 4.1, the values of fluorescence measured with the plate reader.

Table 4.1: Fluorescence values of PCL, 1% PCLM and 10% PCLM

PCL	1% PCLM	10% PCLM
555	540	955
8373	13143	21201

From both results, the samples that were immersed in the solution BSA-FITC/PB buffer show the fluorescence signal, whereas the control samples immersed in PB buffer do not show any fluorescence. The images are confirmed by the values in Table 4.1. The results increase with the introduction and the increment of the percentage of PCL-maleimide. The fluorescence is present also in the PCL sample, in which there is no maleimide. This can be due to the adsorption of the BSA protein on the surface, during the immersion in the PB buffer, but the value is the lowest compared to the samples in which the maleimide is present. Therefore, the fluorescence of the BSA-FITC confirms the presence of the maleimide in the PCLM surfaces, showing a higher value for 10% PCLM.

4.4 PNIPAM brushes

After testing the presence of the maleimide on the surfaces, PNIPAM brushes were added on the following samples:

- PCL
- 1% PCLM
- 10% PCLM

These were analysed with FT-IR, contact angle and using Alkoxyamine-PEG4-Biotin.

4.4.1 FT-IR

The FT-IR spectrum of the PNIPAM M_n=23000 g/mol, with its structure, is shown in Figure 4.7:

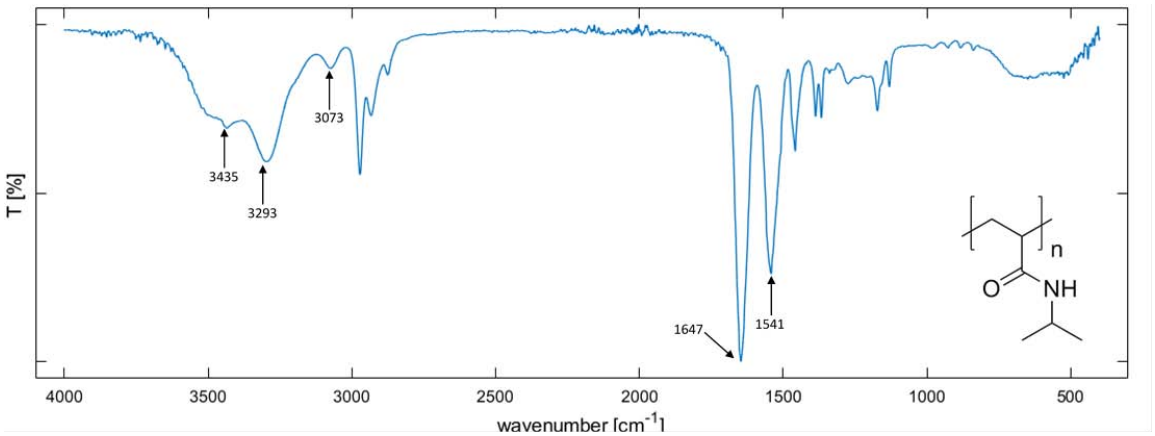

Figure 4.7: FT-IR spectrum of PNIPAM

The principal peaks of PNIPAM are the following:

- N-H stretching in the IR region between 3500-3000 cm^{-1}
- C=O stretching at wavelength 1647 of cm^{-1}
- C-N stretching and N-H bending at wavelength of 1541 cm^{-1} [97]

The surfaces were analysed with FT-IR after the addition of the PNIPAM brushes, obtaining the spectra shown in Figure 4.8.

Compared to the spectrum of only PCL, in Figure 3.3, all the samples + brushes show additional peaks in two IR regions, between 3600-3000 cm^{-1}

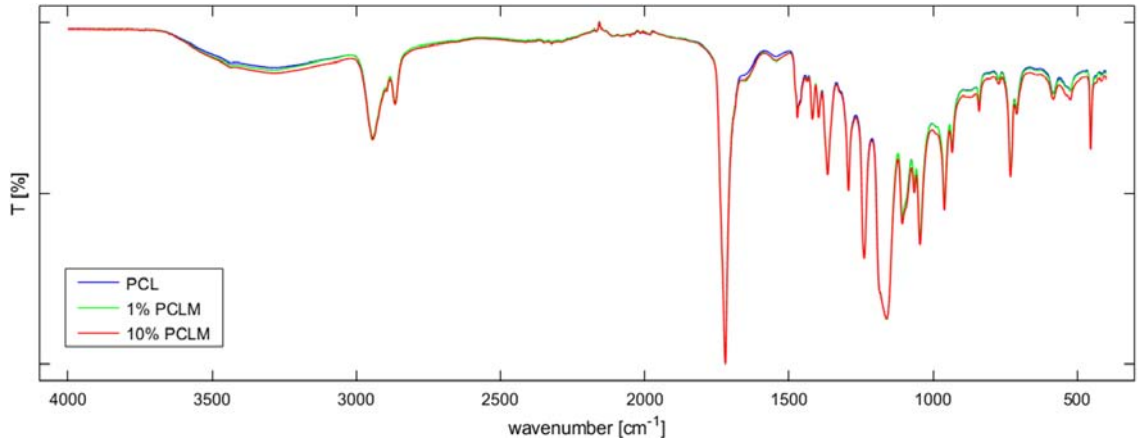

Figure 4.8: FT-IR spectra of PCL, 1% PCLM and 10% PCLM + PNIPAM brushes

and between 1700-1500 cm^{-1}. The changing in the spectra in these regions is evidenced in all the samples, included PCL without the maleimide on the surface. The different profile of the spectrum of PCL can be due to the absorption of PNIPAM on the surface, during the immersion in the solution of brushes in PB buffer, carried out at pH=7. In addition, all the spectra seem to follow the same trend, with minimum differences even between the samples containing PCL-maleimide. From these results, it is not possible to state to which surface the PNIPAM brushes were bound and the experiment was repeated afterwards with the introduction of a catalyst in the solution.

4.5 Biological characterization of PCLM films

After the introduction of the brushes, the samples were immersed in the solution of RGD peptide for a week. In order to show the influence of the different components of the surfaces on the cells, the following samples were seeded with MG 63 osteosarcoma cells:

- Neat surfaces: PCL, 1% PCLM, 10% PCLM
- (PCL, 1% PCLM, 10% PCLM) + PNIPAM brushes
- (PCL, 1% PCLM, 10% PCLM) + PNIPAM brushes + RGD peptide

Then, the cells were fixed and analysed after 1 day and 3 days. The samples were not analysed after 7 days, as for the aminolysed films, because after 7 days, there is a great amount of cells on the surface and this rapid growth does not allow distinguishing the influence of the modification processes on

the films. For this reason, day 3 was chosen as second time point for the analysis.

4.5.1 Day 1

The images of the stained cells are shown in Figure 4.9 and they indicate a portion of each film, representative for the all surface.

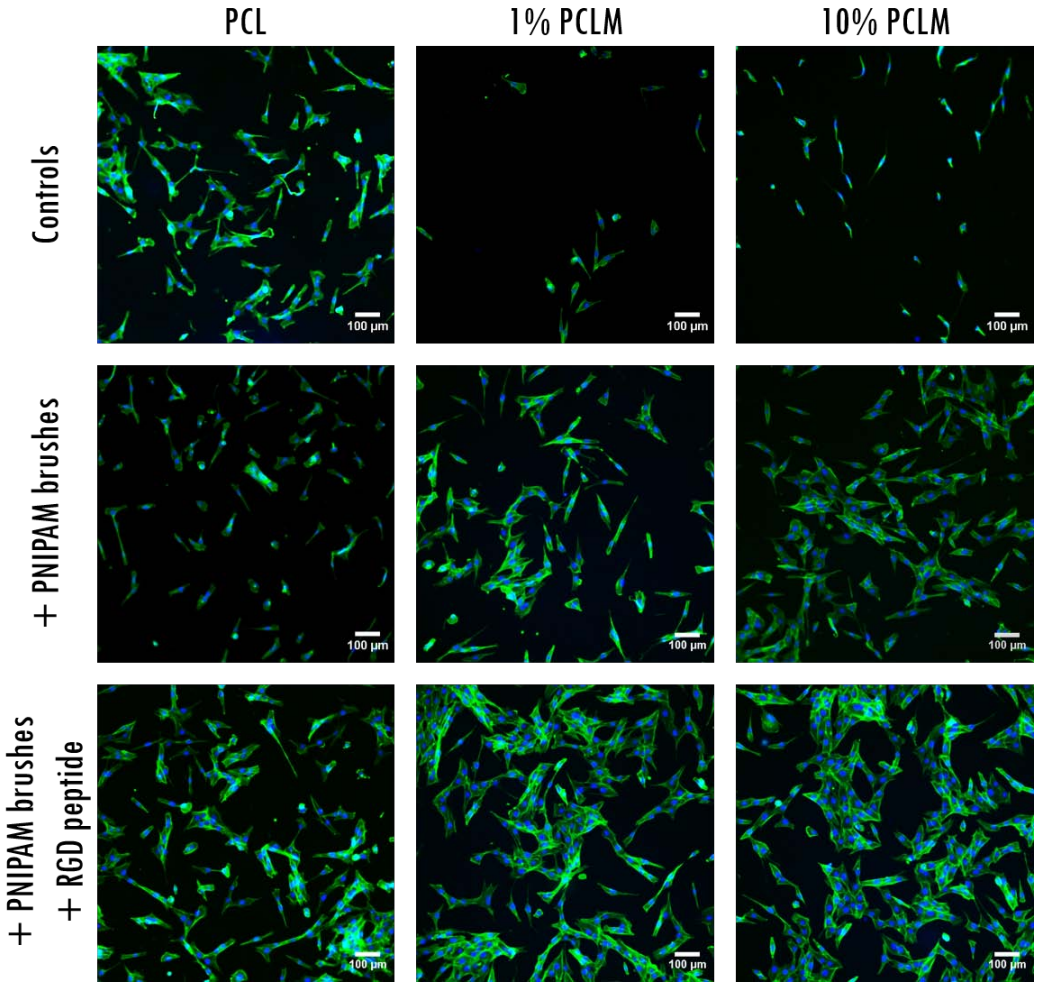

Figure 4.9: Day 1: Phalloidin 488 and DAPI staining of cells on PCL, 1% PCLM and 10% PCLM, + PNIPAM brushes and + PNIPAM bruhes + RGD peptide surfaces

From left to right, there are the different surfaces, while from the top to the bottom, the images represents the cells in contact with different modifica-

tions of the surface.

In addition, the nuclei of the cells were counted with CellProfiler and the result is shown in the graphs in Figure 4.10.

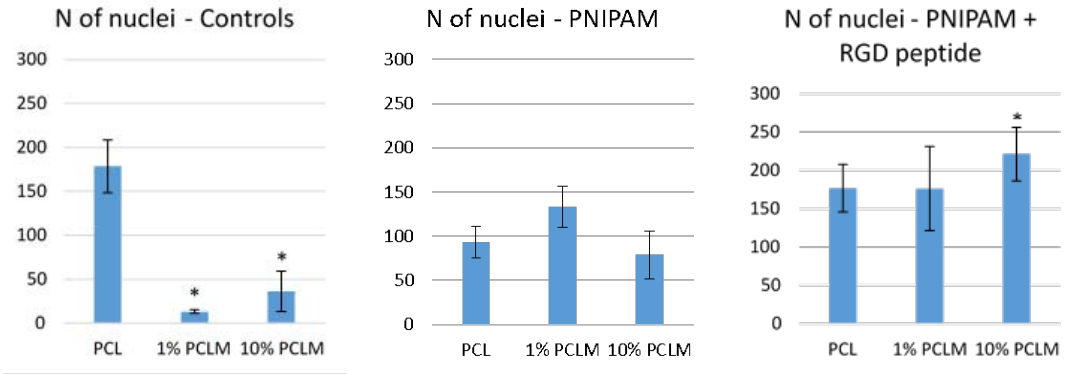

Figure 4.10: Day 1: Number of nuclei for the different conditions

Compared to the control samples, the number of cells increases with the addition of RGD peptide, after 1 day, in the samples with a percentage of maleimide present on the surface. The PCLM samples show an increase of the number of cells after the introduction of PNIPAM brushes; the number is maintained constant after the introduction of RGD peptide for 1% of PCLM, while there is a significant increase for the sample of 10% PCLM, compared to the sample with PNIPAM brushes. The number of cells on PCL surface does not show significant changes during the experiment. Lastly, the maleimide present on the surface decreases significantly the number of cells on the PCLM surfaces compared to the PCL. In this way, it is possible to show the influence on cell adhesion of the different components used in the samples: maleimide, PNIPAM brushes and RGD peptide and compared it with the respective controls.

4.5.2 Day 3

The same seeded samples were analysed after 3 days and the images of DAPI and phalloidin staining of the cells are shown in Figure 4.11. The arrangement of the images is the same of Figure 4.9.

The number of cells on the samples is counted using CellProfiler and the graphs relating to the number of nuclei on the surfaces after 3 days are shown in Figure 4.12.

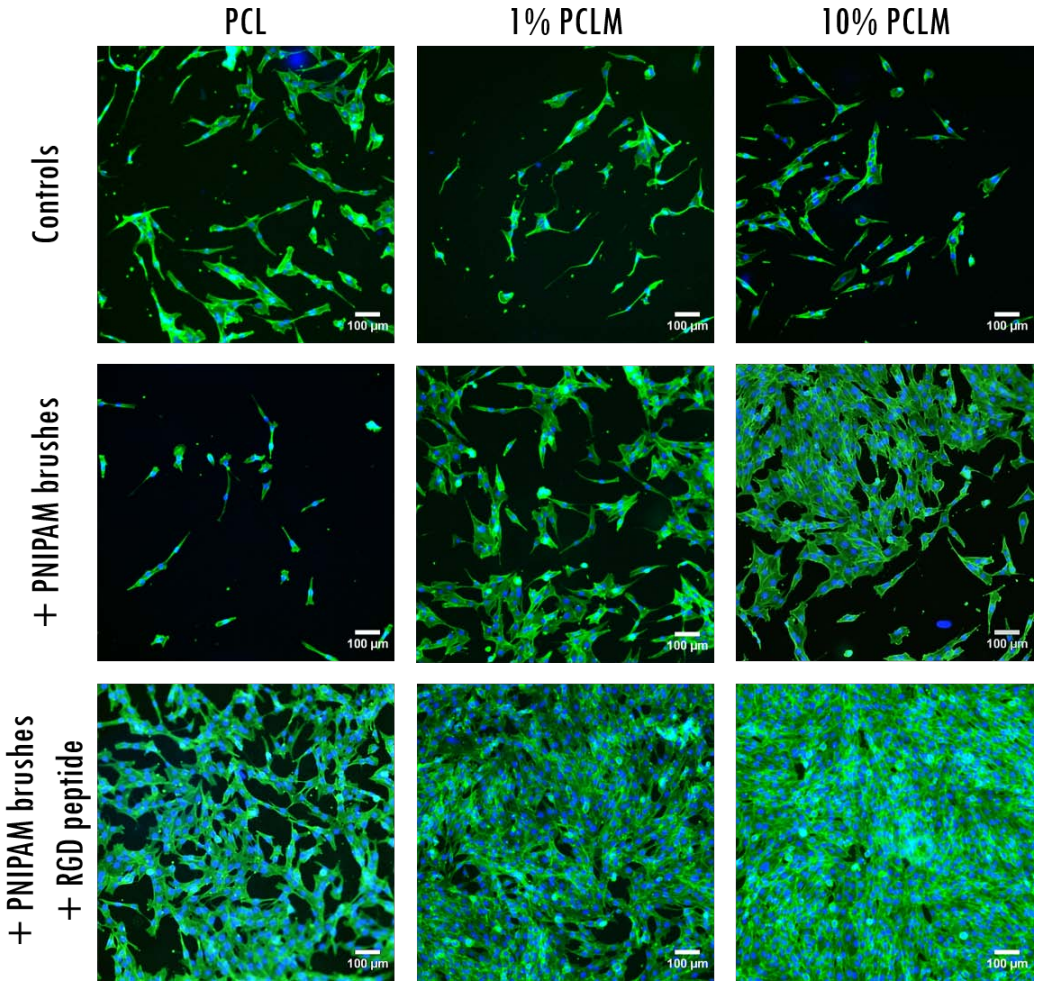

Figure 4.11: Day 3: Phalloidin 488 and DAPI staining of cells on PCL, 1% PCLM and 10% PCLM, + PNIPAM brushes and + PNIPAM bruhes + RGD peptide surfaces

The number of cells on the neat surfaces and after the introduction of PNIPAM brushes follows the trend shown after 1 day, while the number of the cells on the PCLM surfaces after the addition of the RGD peptide is doubled compared with PCL, showing a greater difference between the PCL and the PCLM samples. In particular, a significant increase is shown for the 10% PCLM sample compared to the control and with PNIPAM brushes samples.

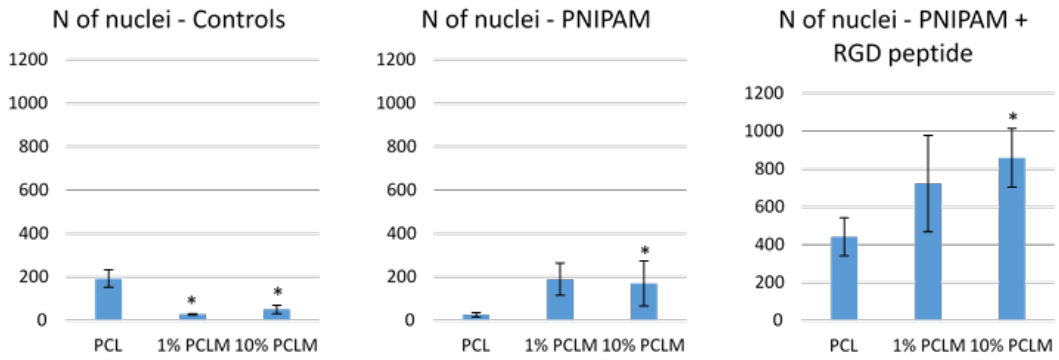

Figure 4.12: Day 3: Number of nuclei for the different conditions

4.6 Optimization of introduction of brushes and peptide

After the analysis described in the previous section, some steps of the procedure were optimized. In particular, the addition of the PNIPAM brushes and the introduction of the RGD peptide were performed using two different catalysts, TEA and *m*-phenylenediamine respectively. This allowed reducing the time of immersion in the solutions of brushes and peptide, and making specific the coupling between the different components added to the surfaces.

4.6.1 Addition of PNIPAM brushes

First, another percentage of PCL-maleimide was introduced, 20% PCLM; therefore, the PNIPAM brushes were added to the following samples:

- PCL
- 1% PCLM
- 10% PCLM
- 20% PCLM

Then, these samples were analysed with FT-IR and, to test the amino-oxy - aldehyde reaction in presence of the catalyst *m*-phenylenediamine, Alkoxyamine-PEG4-Biotin was used.

4.6.1.1 FT-IR

The spectra of the samples after the addition of the PNIPAM brushes are shown in Figure 4.13

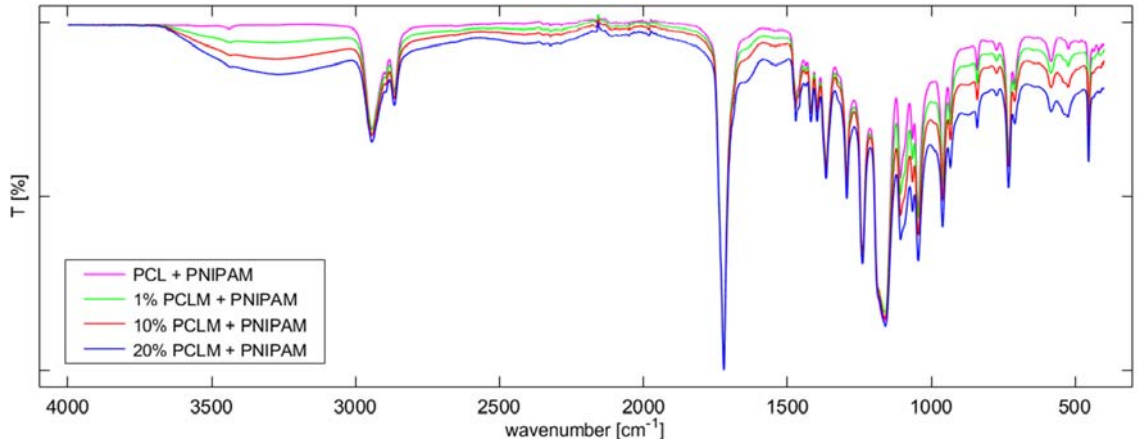

Figure 4.13: FT-IR spectra of PCL, 1% PCLM, 10% PCLM and 20% PCLM + PNIPAM brushes

In this case, the spectrum of the PCL does not change after the immersion in the solution with the polymer brushes, showing only the typical peaks of the material. In the spectra of the PCLM surfaces, increasing peaks appear in two different regions:

- 3700-3000 cm^{-1} region, attributable to N-H stretching
- 1700-1500 cm^{-1} region, in which two peaks are present, attributable to C=O stretching, C-N stretching and N-H bending

The peaks increase with the increasing of the percentage of PLC-maleimide and they are more evident for the 20% of PCLM, in particular in the second IR region. The two peaks, belonging to the IR region between 1700-1500 cm^{-1}, represent the amide peaks and confirm the presence of the PNIPAM on the surface. Gunnewiek et al. also stated the reduction of the ester peaks of the PCL, that in these results was not changing, while the presence of the peak in 3700-3000 cm^{-1} region was not mentioned [98]. These spectra are obtained after the immersion of the samples in a solution of PNIPAM brushes, with the addition of the catalyst TEA. The presence of this catalyst allows the specific coupling of the brushes with the maleimide on the surface and it prevents the adsorption of the brushes on the PCL surface, which does not show different peaks on the spectrum.

4.6.1.2 Alkoxyamine-PEG4-Biotin

Before the introduction of the RGD peptide, the amino-oxy - aldehyde reaction was tested using the specific dye Alkoxyamine-PEG4-Biotin, in presence of *m*-phenylenediamine. The dye was added to the samples with PNIPAM brushes overnight and then analysed using the microscope and measuring the fluorescence with the plate reader.

The fluorescence images of the samples are shown Figure 4.15, compared to the result images of the same dye without the use of the catalyst, Figure 4.14. The images are followed by the measured values of fluorescence in Table 4.2

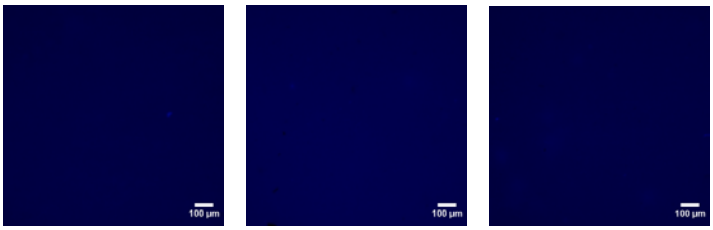

Figure 4.14: Fluorescence images of PCL, 1% PCLM and 10% PCLM + PNIPAM, reaction for 24h

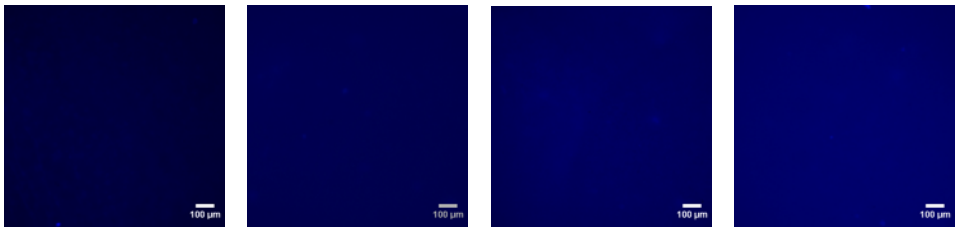

Figure 4.15: Fluorescence images of PCL, 1% PCLM, 10% PCLM and 20% PCLM + PNIPAM, reaction overnight

The images of Figure 4.15 represent the samples with PNIPAM brushes, in which the reaction between the functional groups of the brushes and the dye was performed overnight: it is possible to notice the increasing of blue fluorescence in the samples with increasing percentage of PCL-maleimide. In addition, the PCL samples shows the lowest value of fluorescence in presence of the catalyst. Conversely, the images in Figure 4.14 are the fluorescence results of the samples in which the reaction was performed without the catalyst and for longer time, 24 hours. The values of fluorescence, obtained in this case, are very similar between the samples and lower compared to

Table 4.2: Values of fluorescence of PCL, 1% PCLM, 10% PCLM and 20% PCLM + PNIPAM

(a)

PCL	1% PCLM	10% PCLM
6447	8677	7175

(b)

PCL	1% PCLM	10% PCLM	20% PCLM
13063	17075	18553	22759

the values of Table 4.2(b), making difficult interpreting the results of the reaction.

From these results, it is evident that the presence of the catalyst increases the time of the reaction between the aldehyde group on the PNIPAM brushes and the amino-oxy group present in the Alkoxyamine-PEG4-Biotin. The efficiency of *m*-phenylenediamine in accelerating the reaction under physiological conditions has been reported in literature [99]; in addition, the concentration of *m*-phenylenediamine can be higher compared to other catalysts, due to its superior solubility limit at pH=7 [100].
Testing the samples using Alkoxyamine-PEG4-Biotin allows predicting the link between the PNIPAM brushes and the RGD peptide, containing an amino-oxy group. For further investigations of the coupling between the brushes and the peptide, a small molecule test with compounds containing the two functional groups can be performed.

After this test, RGD peptide was added to the samples, to which PNIPAM brushes were added in presence of TEA, in a solution using the same catalyst employed with the biotin dye. The reaction was performed for two days, followed by the biological characterization of the samples.

4.7 Biological characterization

Therefore, the procedure of cell seeding and staining was repeated with the following samples:

- Neat surfaces: PCL, 1% PCLM, 10% PCLM, 20% PCLM
- (PCL, 1% PCLM, 10% PCLM, 20% PCLM) + PNIPAM brushes
- (PCL, 1% PCLM, 10% PCLM, 20% PCLM) + PNIPAM brushes + RGD peptide

The cells seeded on these samples were fixed, stained and analysed after 1 day and 3 days.

4.7.1 Day 1

The images related to DAPI and phalloidin 488 staining of MG 63 on the different samples after 1 day are shown in Figure 4.16. From left to right, there are the different surfaces, from the top to the bottom, the different modifications of the surface are represented. In addition, the nuclei of the cells were counted and the result is shown in the graphs in Figure 4.17.

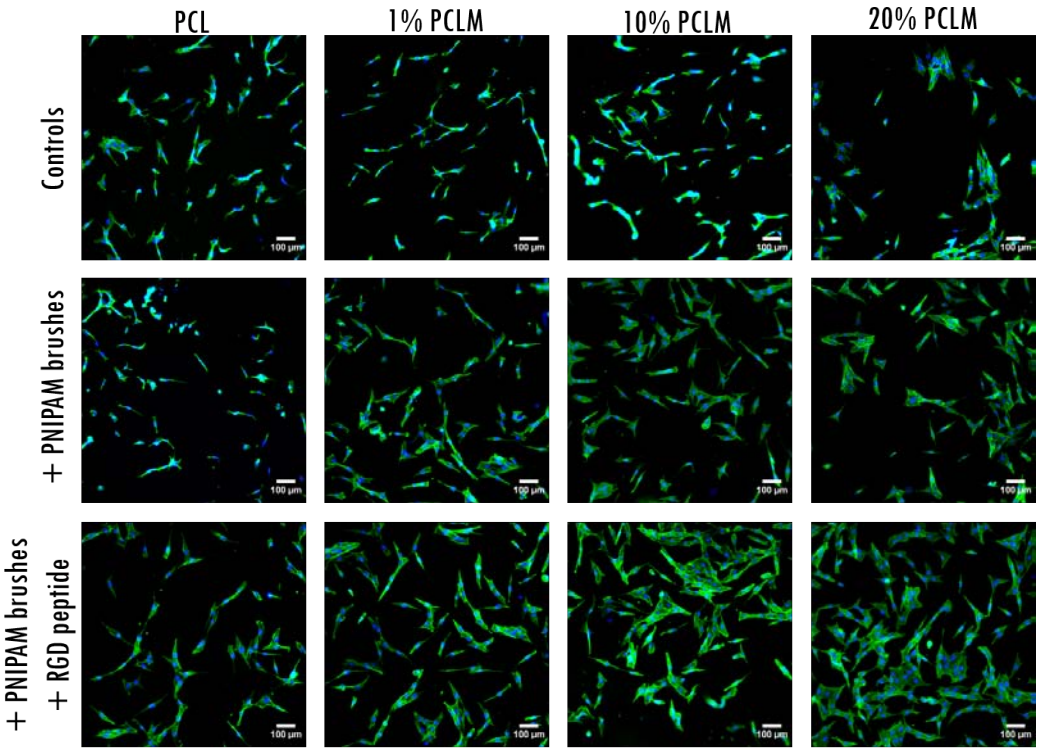

Figure 4.16: Day 1: Phalloidin 488 and DAPI staining of cells on PCL, 1% PCLM, 10% PCLM and 20% PCLM, + PNIPAM brushes and + PNIPAM bruhes + RGD peptide surfaces

The results obtained from the counting of nuclei present in the samples can be compared with the numbers of previous experiments, without the use of catalysts. In this case, the neat surfaces shows similar number of cells after 1 day, even in the samples with the highest percentage of the PCL-maleimide. The same trend is followed for the samples after the introduction of the PNIPAM brushes. The number of cells increases with the introduction of the

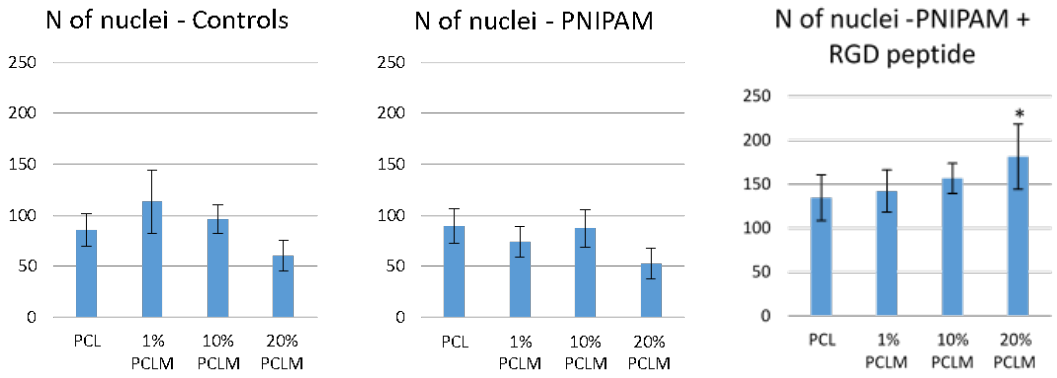

Figure 4.17: Day 1: Number of nuclei for the different conditions

RGD peptide, showing differences between the different samples of PCLM. Compared to previous results (Figure 4.10), the results of these experiment show similar results between the samples, with the addition of the samples with higher percentage of maleimide, that shows a significant increase in presence of RGD peptide compared to control samples. The presence of cells on the surface increases with the increasing of the percentage of the PCL-maleimide, to which the PNIPAM brushes and consequently the RGD peptide are coupled. A greater percentage of maleimide on the surface allow coupling a higher number of PNIPAM brushes, to which more RGD peptide can link. Furthermore, the number of cells on PCL surface remains around the same value during the all experiment.

4.7.2 Day 3

After 3 days, the images of the stained cells are shown in Figure 4.18, with the same arrangement of the images of Figure 4.16, followed by the graphs obtained from the counting with CellProfiler in Figure 4.19.

In this experiment, the number of cells are similar between the samples of neat surfaces and after the addition of the PNIPAM brushes; there is no significant differences between the samples and conditions. The number of nuclei of PCL surface remains almost constant between the different conditions, as shown for day 1. The PCLM samples show a great increase of the cells on the surface with the introduction of the RGD peptide. The value of counted nuclei is double for the 1% PCLM, tripled for the 10% PCLM and it is almost quadrupled for the 20% PCLM, compared to the value for the

neat surfaces and with the PNIPAM brushes. The raise of the cell adhesion on surfaces increases significantly for 10% and 20% of PCL-maleimide. The same trend, shown after 1 day, results more evident after 3 days.

The influence of RGD peptide on cell adhesion is widely reported in literature [50, 51, 101], showing the increasing of the number of cells on different types of surface, functionalized with this bioactive peptide. The cell activity of MG 63 osteosarcoma cells benefits from the immobilization of RGD peptide on a polymer surface as well as on a metal surface [102, 103].

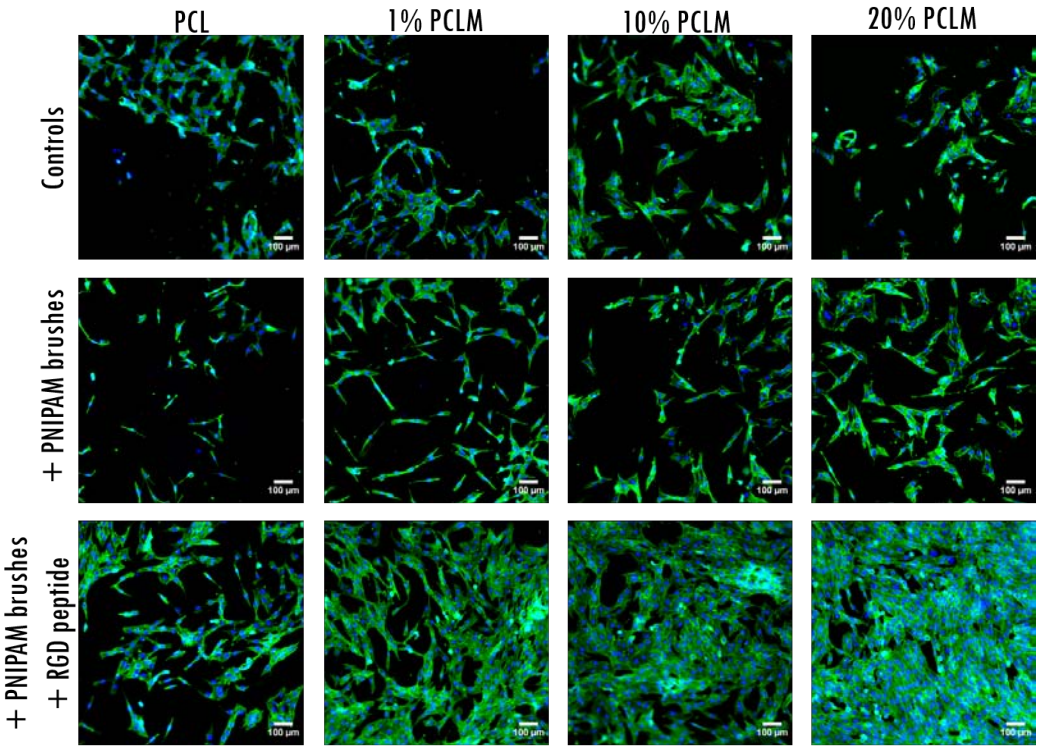

Figure 4.18: Day 3: Phalloidin 488 and DAPI staining of cells on PCL, 1% PCLM, 10% PCLM and 20% PCLM, + PNIPAM brushes and + PNIPAM bruhes + RGD peptide surfaces

From these last results, the presence of RGD peptide increases the cell adhesion on the different PCLM surfaces, increasing the number of cells with the increase of the percentage of PCL-maleimide used to prepare the samples. The usage of catalysts for the addition of the brushes and the peptide allows obtaining a quicker reaction between the different components [99], as reported in section 4.6.1.2 with the use of Alkoxyamine-PEG4-Biotin, and furthermore, a specific coupling between them, as shown in FT-IR spectra in Figure 4.13, in which PCL did not show addition peaks to its spectrum.

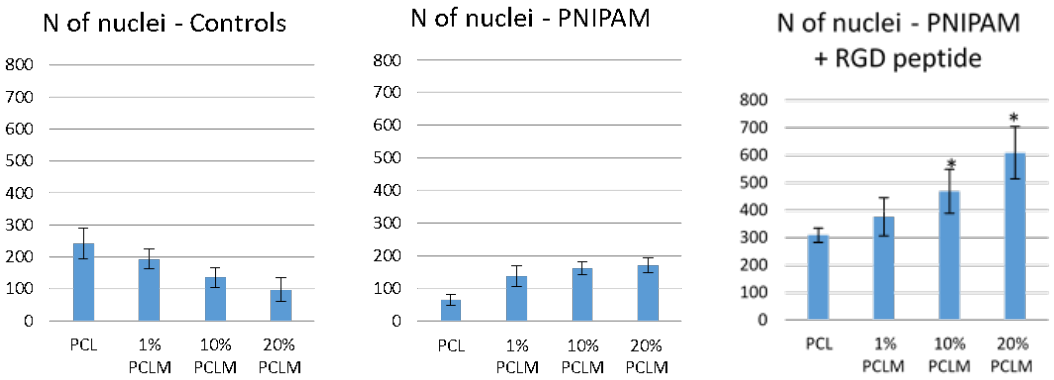

Figure 4.19: Day 3: Number of nuclei for the different conditions

In this way, a higher percentage of maleimide on the surfaces can link to an higher number or PNIPAM brushes, which accordingly can couple to a bigger number of RGD peptide, bringing to an increase of the cell adhesion on the surface, proved by the images of the staining and the counting of the nuclei.

Chapter 5

Conclusions

In this thesis project, the main focus is the functionalization of PCL films with RGD peptide, through the specific coupling with polymer brushes, made of PNIPAM. The first step to achieve this goal was the preparation and test of the surfaces, starting from pure PCL to the introduction of maleimide.

The first modification of the surface via aminolysis showed increasing cell adhesion to the surface, as known from literature. Furthermore, it was determined the optimal duration of the reaction, 1 hour, to obtain higher signal from the reaction between the polyester and the amino groups. More research is needed to understand the outcome obtained from the ninhydrin assay and why it differs from the results shown in literature papers.

After this first step, commercial available PCL of M_n=45,000 was mixed using the extruder with synthetized PCL-maleimide and afterwards, films were made out of it. These samples were obtaining using the hot press, which is a method similar to printing. In addition, after the mixing, the presence of the maleimide on the surfaces was confirmed by the analysis with BSA-FITC. These information can be useful for further applications of this mixed material.

The last and most important step of this work is represented by the introduction of the PNIPAM brushes on the surface and the succeeding functionalization with the RGD peptide. After the first trial, the samples seeded with MG 63 cells showed an increasing adhesion on the surface in presence of PNIPAM brushes functionalized with RGD peptide, although the surfaces with different percentage of maleimide showed similar results. In this case, the positive effect on the RGD peptide on the cells was shown.

To improve the functionalization of the surfaces, two catalysts were introduced. In this way, it was possible to optimize the introduction of the PNIPAM brushes, as shown in the FT-IR spectra, with increasing signal as percentages of PCL-maleimide increase. This result shows the successful introduction of the PNIPAM brushes on the different surfaces, except on the PCL surface, where there is no maleimide available on the surface. In addition, the presence of TEA catalyst allowed reducing the time of the reaction between the maleimide and the brushes, making the reaction faster and avoiding the absorption of the brushes on the surface.

Moreover, in presence of *m*-phenylenediamine better results were shown for the reaction between the aldehyde group on the brushes and the amino-oxy group present on the peptide. Also in this case, the use of the catalyst increases the time of the reaction, avoiding not only the absorption of the peptide on the surface, but also the possible damage of the peptide for longer reaction. The test using the Alkoxyamine-PEG4-Biotin showed the successful coupling between the functional group of the PNIPAM brushes and the RGD peptide.

To achieve the building of this surface functionalization of PCL, maleimide, PNIPAM brushes and RGD peptide, the possibility of introducing precise functional groups on these compounds was fundamental. The use of the specific RAFT agent for the PNIPAM brushes and the preparation of the peptide with an amino-oxy group allowed the specific coupling between maleimide and brushes, and between the brushes and the RGD peptide.

Finally, the samples were seeded with MG63 cells and the increase of the cell adhesion was showed in samples with PNIPAM brushes functionalized with RGD peptide; this result was better shown after 3 days of cell culture on the surfaces.

In conclusion, the successful outcomes of this thesis work can be summarized as follows:

- Preparation of PCL films with maleimide on the surface
- Preparation of PNIPAM brushes and RGD peptide with relevant functional groups
- Introduction of PNIPAM brushes on PCL-maleimide surfaces
- Functionalization of brushes with RGD peptide via aldehyde-amino-oxy reaction
- Increase of cell adhesion in response to RGD peptide

This thesis work is only the first step in the functionalization of PCL using brushes and RGD peptide. Further researches and tests on the reactions between the different compounds and on the conditions of the reactions have to be performed. Various types of polymer brushes and peptides can be tested to achieve different outcomes. In addition, the cells used can be changed in favour of human mesenchymal stromal cells (hMSCs) for future studies of proliferation, adhesion and differentiation. All the samples in this project are represented 2D surfaces: after the studies on these samples, future works are needed for the transition to 3D scaffolds.

Appendix A

Abbreviations

AIBN = Azobisisobutyronitrile
Aoa = amino-oxy-acetic acid
BSA - FITC = Albumin-fluorescein isothiocyanate conjugate
BSA = Bovine serum albumin
DAPI = 4',6-Diamidino-2-phenylindole dihydrochloride
DMF = N,N-dimethylformamide
DMSO = Dimethyl sulfoxide
EDTA = Ethylenediaminetetraacetic acid
FBS = Fetal bovine serum
LiBr = Lithium bromide
MEM α-= Minimum essential medium α
NaOH = Sodium hydroxide
NIPAM = N-Isopropylacrylamide
PBS = Phosphate buffered saline
PCL = Polycaprolactone
PEG = Polyethylene glycol
PFA = Paraformaldehyde
PNIPAM = Poly(N-isopropylacrylamide)
PTFE = Polytetrafluoroethylene
TCEP = Tris(2-carboxyethyl)phosphine hydrochloride)
TEA = Triethylamine

Bibliography

[1] EB Hunziker. Articular cartilage repair: basic science and clinical progress. a review of the current status and prospects. *Osteoarthritis and cartilage*, 10(6):432–463, 2002.

[2] Michael Keeney, Janice H Lai, and Fan Yang. Recent progress in cartilage tissue engineering. *Current opinion in biotechnology*, 22(5):734–740, 2011.

[3] Nora T Khanarian, Jie Jiang, Leo Q Wan, Van C Mow, and Helen H Lu. A hydrogel-mineral composite scaffold for osteochondral interface tissue engineering. *Tissue Engineering Part A*, 18(5-6):533–545, 2011.

[4] David T Felson, Reva C Lawrence, Paul A Dieppe, Rosemarie Hirsch, Charles G Helmick, Joanne M Jordan, Raynard S Kington, Nancy E Lane, Michael C Nevitt, Yuqing Zhang, et al. Osteoarthritis: new insights. part 1: the disease and its risk factors. *Annals of internal medicine*, 133(8):635–646, 2000.

[5] Johannes WJ Bijlsma, Francis Berenbaum, and Floris PJG Lafeber. Osteoarthritis: an update with relevance for clinical practice. *The Lancet*, 377(9783):2115–2126, 2011.

[6] Sarah R Kingsbury, Hillary J Gross, Gina Isherwood, and Philip G Conaghan. Osteoarthritis in europe: impact on health status, work productivity and use of pharmacotherapies in five european countries. *Rheumatology*, 53(5):937–947, 2014.

[7] Sion Glyn-Jones, AJR Palmer, R Agricola, AJ Price, TL Vincent, H Weinans, and AJ Carr. Osteoarthritis. *The Lancet*, 386(9991):376–387, 2015.

[8] Sven Knecht, Benedicte Vanwanseele, and Edgar Stüssi. A review on the mechanical quality of articular cartilage–implications for the

diagnosis of osteoarthritis. *Clinical biomechanics*, 21(10):999–1012, 2006.

[9] Brian Wu. Stages of osteoarthritis of the knee. https://www.medicalnewstoday.com/kc/stages-osteoarthritis-knee-310579.

[10] Buddy D Ratner, Allan S Hoffman, Frederick J Schoen, and Jack E Lemons. *Biomaterials science: an introduction to materials in medicine*. Academic press, 2004.

[11] Stephen Corteen Cowin et al. *Bone mechanics handbook*. CRC press, 2001.

[12] Wikimedia Commons. File:bone cross-section.svg — wikimedia commons, the free media repository, 2017.

[13] Andrea Di Luca, Clemens Van Blitterswijk, and Lorenzo Moroni. The osteochondral interface as a gradient tissue: From development to the fabrication of gradient scaffolds for regenerative medicine. *Birth Defects Research Part C: Embryo Today: Reviews*, 105(1):34–52, 2015.

[14] Rinaldo Florencio-Silva, Gisela Rodrigues da Silva Sasso, Estela Sasso-Cerri, Manuel Jesus Simões, and Paulo Sérgio Cerri. Biology of bone tissue: structure, function, and factors that influence bone cells. *BioMed research international*, 2015, 2015.

[15] Brian K Hall. *Bones and cartilage: developmental and evolutionary skeletal biology*. Academic Press, 2005.

[16] Alice J Sophia Fox, Asheesh Bedi, and Scott A Rodeo. The basic science of articular cartilage: structure, composition, and function. *Sports health*, 1(6):461–468, 2009.

[17] Kyriacos A Athanasiou, Eric M Darling, and Jerry C Hu. Articular cartilage tissue engineering. *Synthesis Lectures on Tissue Engineering*, 1(1):1–182, 2009.

[18] F Berenbaum. Osteoarthritis as an inflammatory disease (osteoarthritis is not osteoarthrosis!). *Osteoarthritis and Cartilage*, 21(1):16–21, 2013.

[19] Joseph A Buckwalter, Van C Mow, and Anthony Ratcliffe. Restoration of injured or degenerated articular cartilage. *Journal of the American Academy of Orthopaedic Surgeons*, 2(4):192–201, 1994.

[20] Abhijit M Bhosale and James B Richardson. Articular cartilage: structure, injuries and review of management. *British medical bulletin*, 87(1):77–95, 2008.

[21] Timothy M O'Shea and Xigeng Miao. Bilayered scaffolds for osteochondral tissue engineering. *Tissue Engineering Part B: Reviews*, 14(4):447–464, 2008.

[22] Robert M Nerem and Athanassios Sambanis. Tissue engineering: from biology to biological substitutes. *Tissue engineering*, 1(1):3–13, 1995.

[23] Catherine P Barnes, Scott A Sell, Eugene D Boland, David G Simpson, and Gary L Bowlin. Nanofiber technology: designing the next generation of tissue engineering scaffolds. *Advanced drug delivery reviews*, 59(14):1413–1433, 2007.

[24] Scott J Hollister. Porous scaffold design for tissue engineering. *Nature materials*, 4(7):518, 2005.

[25] Robert Langer and Joseph P. Vacanti. Tissue engineering. *Science*, 260(5110):920–926, 1993.

[26] E Sachlos, JT Czernuszka, et al. Making tissue engineering scaffolds work. review: the application of solid freeform fabrication technology to the production of tissue engineering scaffolds. *Eur Cell Mater*, 5(29):39–40, 2003.

[27] Fergal J O'brien. Biomaterials & scaffolds for tissue engineering. *Materials today*, 14(3):88–95, 2011.

[28] Nicole E Zander, Joshua A Orlicki, Adam M Rawlett, and Thomas P Beebe Jr. Quantification of protein incorporated into electrospun polycaprolactone tissue engineering scaffolds. *ACS applied materials & interfaces*, 4(4):2074–2081, 2012.

[29] J Lannutti, Darrell Reneker, Tea Ma, D Tomasko, and D Farson. Electrospinning for tissue engineering scaffolds. *Materials Science and Engineering: C*, 27(3):504–509, 2007.

[30] C Csaki, PRA Schneider, and M Shakibaei. Mesenchymal stem cells as a potential pool for cartilage tissue engineering. *Annals of Anatomy-Anatomischer Anzeiger*, 190(5):395–412, 2008.

[31] Waradda Mattanavee, Orawan Suwantong, Songchan Puthong, Tanom Bunaprasert, Voravee P Hoven, and Pitt Supaphol. Immobilization of biomolecules on the surface of electrospun polycaprolactone fibrous scaffolds for tissue engineering. *ACS applied materials & interfaces*, 1(5):1076–1085, 2009.

[32] Chester J Koh and Anthony Atala. Tissue engineering, stem cells, and cloning: opportunities for regenerative medicine. *Journal of the American Society of Nephrology*, 15(5):1113–1125, 2004.

[33] Huina Zhang and Scott Hollister. Comparison of bone marrow stromal cell behaviors on poly (caprolactone) with or without surface modification: studies on cell adhesion, survival and proliferation. *Journal of Biomaterials Science, Polymer Edition*, 20(14):1975–1993, 2009.

[34] Bret D Ulery, Lakshmi S Nair, and Cato T Laurencin. Biomedical applications of biodegradable polymers. *Journal of polymer science Part B: polymer physics*, 49(12):832–864, 2011.

[35] Alba C Luca, Giorgio Terenghi, and Sandra Downes. Chemical surface modification of poly-ε-caprolactone improves schwann cell proliferation for peripheral nerve repair. *Journal of tissue engineering and regenerative medicine*, 8(2):153–163, 2014.

[36] Tim Desmet, Thomas Billiet, Elke Berneel, Ria Cornelissen, David Schaubroeck, Etienne Schacht, and Peter Dubruel. Post-plasma grafting of aema as a versatile tool to biofunctionalise polyesters for tissue engineering. *Macromolecular bioscience*, 10(12):1484–1494, 2010.

[37] Maria Ann Woodruff and Dietmar Werner Hutmacher. The return of a forgotten polymer-polycaprolactone in the 21st century. *Progress in polymer science*, 35(10):1217–1256, 2010.

[38] Shaojun Yuan, Gordon Xiong, Ariel Roguin, and Cleo Choong. Immobilization of gelatin onto poly (glycidyl methacrylate)-grafted polycaprolactone substrates for improved cell–material interactions. *Biointerphases*, 7(1-4):30, 2012.

[39] Matthew Tirrell, Efrosini Kokkoli, and Markus Biesalski. The role of surface science in bioengineered materials. *Surface Science*, 500(1):61–83, 2002.

[40] Lorenzo Moroni, Michel Klein Gunnewiek, and Edmondo M Benetti. Polymer brush coatings regulating cell behavior: Passive interfaces turn into active. *Acta biomaterialia*, 10(6):2367–2378, 2014.

[41] Julie Melissa Goddard and JH Hotchkiss. Polymer surface modification for the attachment of bioactive compounds. *Progress in polymer science*, 32(7):698–725, 2007.

[42] Bogdan Zdyrko and Igor Luzinov. Polymer brushes by the "grafting to" method. *Macromolecular rapid communications*, 32(12):859–869, 2011.

[43] William J Brittain and Sergiy Minko. A structural definition of polymer brushes. *Journal of Polymer Science Part A: Polymer Chemistry*, 45(16):3505–3512, 2007.

[44] Steve Edmondson, Vicky L Osborne, and Wilhelm TS Huck. Polymer brushes via surface-initiated polymerizations. *Chemical society reviews*, 33(1):14–22, 2004.

[45] Mahentha Krishnamoorthy, Shoghik Hakobyan, Madeleine Ramstedt, and Julien E Gautrot. Surface-initiated polymer brushes in the biomedical field: applications in membrane science, biosensing, cell culture, regenerative medicine and antibacterial coatings. *Chemical reviews*, 114(21):10976–11026, 2014.

[46] Bin Zhao and William J Brittain. Polymer brushes: surface-immobilized macromolecules. *Progress in Polymer Science*, 25(5):677–710, 2000.

[47] Jenny E Raynor, Jeffrey R Capadona, David M Collard, Timothy A Petrie, and Andrés J García. Polymer brushes and self-assembled monolayers: versatile platforms to control cell adhesion to biomaterials. *Biointerphases*, 4(2):FA3–FA16, 2009.

[48] Woonjung Kim and Jongjin Jung. Polymer brush: a promising grafting approach to scaffolds for tissue engineering. *BMB reports*, 49(12):655, 2016.

[49] Xiaofeng Sui, Szczepan Zapotoczny, Edmondo M Benetti, Peter Schön, and G Julius Vancso. Characterization and molecular engineering of surface-grafted polymer brushes across the length scales by atomic force microscopy. *Journal of materials chemistry*, 20(24):4981–4993, 2010.

[50] Keun-Hong Park, Kun Na, and Hyung-Min Chung. Enhancement of the adhesion of fibroblasts by peptide containing an arg-gly-asp sequence with poly (ethylene glycol) into a thermo-reversible hydrogel as a synthetic extracellular matrix. *Biotechnology letters*, 27(4):227–231, 2005.

[51] Ulrich Hersel, Claudia Dahmen, and Horst Kessler. Rgd modified polymers: biomaterials for stimulated cell adhesion and beyond. *Biomaterials*, 24(24):4385–4415, 2003.

[52] Michael D Pierschbacher and Erkki Ruoslahti. Cell attachment activity of fibronectin can be duplicated by small synthetic fragments of the molecule. *Nature*, 309(5963):30–33, 1984.

[53] PepBank. Grgdsp. `http://pepbank.mgh.harvard.edu/interactions/details/18448`.

[54] John Coates. Interpretation of infrared spectra, a practical approach. *Encyclopedia of analytical chemistry*, 2000.

[55] WD Perkins. Fourier transform-infrared spectroscopy: Part l. instrumentation. *J. Chem. Educ*, 63(1):A5, 1986.

[56] Donald L Pavia, Gary M Lampman, George S Kriz, and James A Vyvyan. *Introduction to spectroscopy*. Cengage Learning, 2008.

[57] Shiqi Wang. Gel permeation chromatography/ size exclusion chromatography, 2014. `https://itn-snal.net/2014/11/gel-permeation-chromatography-size-exclusion-chromatography/`.

[58] Carlo Di Bello. *Biomateriali: introduzione allo studio dei materiali per uso biomedico*. Pàtron, 2004.

[59] Wikimedia Commons. File:contact angle.svg — wikimedia commons, the free media repository, 2015. `https://commons.wikimedia.org/w/index.php?title=File:Contact_angle.svg&oldid=178863538`.

[60] Thermo Fisher Scientific. Cell culture basics handbook. *UK: Gibco*, 2015.

[61] Tamara Straube, Claudia Müller. How to do a proper cell culture quick check, 2016. `http://www.leica-microsystems.com/science-lab/how-to-do-a-proper-cell-culture-quick-check/`.

[62] Jan Kapuscinski. Dapi: a dna-specific fluorescent probe. *Biotechnic & Histochemistry*, 70(5):220–233, 1995.

[63] Thermo-Fisher Scientific. Dapi (4',6-diamidino-2-phenylindole, dihydrochloride). `https://www.thermofisher.com/order/catalog/product/D1306`.

[64] Brad Chazotte. Labeling nuclear dna using dapi. *Cold Spring Harbor Protocols*, 2011(1):pdb–prot5556, 2011.

[65] Christoph Greb. Fluorescent dyes, an overview, 2012. `http://www.leica-microsystems.com/science-lab/fluorescent-dyes/`.

[66] Thermo-Fisher Scientific. Phalloidin conjugates for staining actin. `https://www.thermofisher.com/it/en/home/life-science/cell-analysis/cell-structure/cytoskeleton/phalloidin-and-phalloidin-conjugates-for-staining-actin.html`.

[67] Thermo-Fisher Scientific. Alexa fluor™ 488 phalloidin. `https://www.thermofisher.com/order/catalog/product/A12379?SID=srch-srp-A12379`.

[68] Thermo-Fisher Scientific. Bovine pulmonary artery endothelial cells stained with alexa fluor® 488 phalloidin and dapi. `https://www.thermofisher.com/it/en/home/technical-resources/research-tools/image-gallery/image-gallery-detail.2183.html`.

[69] Yang Zhu, Zhengwei Mao, and Changyou Gao. Aminolysis-based surface modification of polyesters for biomedical applications. *Rsc Advances*, 3(8):2509–2519, 2013.

[70] Yabin Zhu, Changyou Gao, Xingyu Liu, and Jiacong Shen. Surface modification of polycaprolactone membrane via aminolysis and biomacromolecule immobilization for promoting cytocompatibility of human endothelial cells. *Biomacromolecules*, 3(6):1312–1319, 2002.

[71] Yang Zhu, ZhengWei Mao, HuaYu Shi, and ChangYou Gao. In-depth study on aminolysis of poly (ε-caprolactone): Back to the fundamentals. *Science China Chemistry*, 55(11):2419–2427, 2012.

[72] Shaojun Yuan, Gordon Xiong, Xiaoyan Wang, Sam Zhang, and Cleo Choong. Surface modification of polycaprolactone substrates using

collagen-conjugated poly (methacrylic acid) brushes for the regulation of cell proliferation and endothelialisation. *Journal of Materials Chemistry*, 22(26):13039–13049, 2012.

[73] Mendel Friedman. Applications of the ninhydrin reaction for analysis of amino acids, peptides, and proteins to agricultural and biomedical sciences. *Journal of agricultural and food chemistry*, 52(3):385–406, 2004.

[74] Bikshandarkoil R Srinivasan. On the existence of ethylenediaminetetraacetic acid (edta) doped zinc sulphate heptahydrate crystal. *arXiv preprint arXiv:1506.04296*, 2015.

[75] Anica Lankuški, Sébastien Fort, and Frédéric Bossard. Electrospun azido-pcl nanofibers for enhanced surface functionalization by click chemistry. *ACS applied materials & interfaces*, 4(12):6499–6504, 2012.

[76] Maureen A Harrison and Ian F Rae. *General techniques of cell culture*. Cambridge University Press, 1997.

[77] Trypan blue, product page. `http://www.sigmaaldrich.com/catalog/product/aldrich/302643?lang=en&region=NL`.

[78] Warren Strober. Trypan blue exclusion test of cell viability. *Current protocols in immunology*, pages A3–B, 2001.

[79] Oscar Bastidas. Cell counting with neubauer chamber, basic hemocytometer usage. *Celeromics*, 2013.

[80] Johannes Schindelin, Ignacio Arganda-Carreras, Erwin Frise, Verena Kaynig, Mark Longair, Tobias Pietzsch, Stephan Preibisch, Curtis Rueden, Stephan Saalfeld, Benjamin Schmid, et al. Fiji: an open-source platform for biological-image analysis. *Nature methods*, 9(7):676–682, 2012.

[81] Lee Kamentsky, Thouis R Jones, Adam Fraser, Mark-Anthony Bray, David J Logan, Katherine L Madden, Vebjorn Ljosa, Curtis Rueden, Kevin W Eliceiri, and Anne E Carpenter. Improved structure, function and compatibility for cellprofiler: modular high-throughput image analysis software. *Bioinformatics*, 27(8):1179–1180, 2011.

[82] Wikimedia Commons. File:maleimide.png — wikimedia commons, the free media repository, 2016.

[83] Tatsuya Saito, Yusuke Aizawa, Kenji Tajima, Takuya Isono, and Toshifumi Satoh. Organophosphate-catalyzed bulk ring-opening polymerization as an environmentally benign route leading to block copolyesters, end-functionalized polyesters, and polyester-based polyurethane. *Polymer chemistry*, 6(24):4374–4384, 2015.

[84] Rheology Solutions. Thermo scientific haake minictw. `http://www.rheologysolutions.com/thermo-scientific-haake-minictw/`.

[85] Sigma-Aldrich. Albumin, fluorescein isothiocyanate conjugate from bovine, product information sheet. `https://www.sigmaaldrich.com/content/dam/sigma-aldrich/docs/Sigma/Product_Information_Sheet/a9771pis.pdf`.

[86] Daniela Kretschy, Gunda Koellensperger, and Stephan Hann. Elemental labelling combined with liquid chromatography inductively coupled plasma mass spectrometry for quantification of biomolecules: A review. *Analytica chimica acta*, 750:98–110, 2012.

[87] John Chiefari, YK Chong, Frances Ercole, Julia Krstina, Justine Jeffery, Tam PT Le, Roshan TA Mayadunne, Gordon F Meijs, Catherine L Moad, Graeme Moad, et al. Living free-radical polymerization by reversible addition- fragmentation chain transfer: the raft process. *Macromolecules*, 31(16):5559–5562, 1998.

[88] Graeme Moad, Ezio Rizzardo, and San H Thang. Raft polymerization and some of its applications. *Chemistry–An Asian Journal*, 8(8):1634–1644, 2013.

[89] Alexander W Jackson and David A Fulton. Dynamic covalent diblock copolymers prepared from raft generated aldehyde and alkoxyamine end-functionalized polymers. *Macromolecules*, 43(2):1069–1075, 2009.

[90] Thermo-Fisher Scientific. Biotinylation - carbonyls. `https://www.thermofisher.com/it/en/home/life-science/protein-biology/protein-biology-learning-center/protein-biology-resource-library/pierce-protein-methods/biotinylation.html`.

[91] Isaac S Carrico. Chemoselective modification of proteins: hitting the target. *Chemical Society Reviews*, 37(7):1423–1431, 2008.

[92] Sigma-Aldrich. Purpald® - technical bulletin. `http://www.sigmaaldrich.com/content/dam/sigma-aldrich/docs/Aldrich/Bulletin/162892bul.pdf`.

[93] Young-Hee Kim, Md Anirban Jyoti, and Ho-Yeon Song. Immobilization of cross linked col-i–opn bone matrix protein on aminolysed pcl surfaces enhances initial biocompatibility of human adipogenic mesenchymal stem cells (hadmsc). *Applied Surface Science*, 303:97–106, 2014.

[94] Huina Zhang, Chia-Ying Lin, and Scott J Hollister. The interaction between bone marrow stromal cells and rgd-modified three-dimensional porous polycaprolactone scaffolds. *Biomaterials*, 30(25):4063–4069, 2009.

[95] Menemşe Gümüşderelioğlu, Ayşe Karakeçili, and T Tolga Demirtaş. Osteogenic activities of mc3t3-e1 cells on heparin-immobilized poly (caprolactone) membranes. *Journal of Bioactive and Compatible Polymers*, 26(3):257–269, 2011.

[96] Hanna Bramfeldt and Patrick Vermette. Enhanced smooth muscle cell adhesion and proliferation on protein-modified polycaprolactone-based copolymers. *Journal of Biomedical Materials Research Part A*, 88(2):520–530, 2009.

[97] Bingjie Sun, Yinan Lin, and Peiyi Wu. Structure analysis of poly (n-isopropylacrylamide) using near-infrared spectroscopy and generalized two-dimensional correlation infrared spectroscopy. *Applied spectroscopy*, 61(7):765–771, 2007.

[98] Michel Klein Gunnewiek, Andrea Di Luca, Xiaofeng Sui, Clemens A van Blitterswijk, Lorenzo Moroni, and G Julius Vancso. Controlled surface initiated polymerization of n-isopropylacrylamide from polycaprolactone substrates for regulating cell attachment and detachment. *Israel journal of chemistry*, 52(3-4):339–346, 2012.

[99] Mohammad Rashidian, Mohammad M Mahmoodi, Rachit Shah, Jonathan K Dozier, Carston R Wagner, and Mark D Distefano. A highly efficient catalyst for oxime ligation and hydrazone–oxime exchange suitable for bioconjugation. *Bioconjugate chemistry*, 24(3):333–342, 2013.

[100] Michaela Wendeler, Luba Grinberg, Xiangyang Wang, Philip E Dawson, and Manuel Baca. Enhanced catalysis of oxime-based bioconjugations by substituted anilines. *Bioconjugate chemistry*, 25(1):93–101, 2013.

[101] Shyam Patel, Jonathan Tsang, Gregory M Harbers, Kevin E Healy, and Song Li. Regulation of endothelial cell function by grgdsp peptide grafted on interpenetrating polymers. *Journal of Biomedical Materials Research Part A*, 83(2):423–433, 2007.

[102] Promita Bhattacharjee, Deboki Naskar, Hae-Won Kim, Tapas K Maiti, Debasis Bhattacharya, and Subhas C Kundu. Non-mulberry silk fibroin grafted pcl nanofibrous scaffold: promising ecm for bone tissue engineering. *European Polymer Journal*, 71:490–509, 2015.

[103] Shih-Kuang Hsu, Wen-Fu Ho, Shih-Ching Wu, Yun-Shan Chen, and Hsueh-Chuan Hsu. In vitro study of ti-nb-sn alloy surface modified with rgd peptide. *Thin Solid Films*, 620:139–144, 2016.